

Data-Efficient Training by Evolved Sampling

Ziheng Cheng*

Zhong Li[†]

Jiang Bian[‡]

Abstract

Data selection is designed to accelerate learning with preserved performance. To achieve this, a fundamental thought is to identify informative data samples with significant contributions to the training. In this work, we propose **Evolved Sampling (ES)**, a simple yet effective framework for *dynamic* sampling along the training process. This method conducts *batch* level data selection based on the dynamics of losses and augmented *loss differences*, which enables flexible *frequency tuning*, and hence significantly reduces the back propagation time with maintained model performance. Due to its conciseness, ES is also readily extensible to incorporate *set* level data selection (to form ES with pruning, **ESWP**) for further accelerations. As a plug-and-play framework, ES(WP) consistently achieves lossless training accelerations across various pre-training and post-training tasks, saving up to nearly 45% wall-clock time. Our results motivate further investigations on the data efficiency aspect of modern large-scale machine learning.

1 Introduction

Deep learning has showcased remarkable performance across a variety of real-world applications, particularly leading to unparalleled successes of large “foundation” models (Touvron et al. [2023]; Rombach et al. [2022]). On the other hand, since these large models are usually trained on web-scale datasets, the overall computation and memory loads are considerably increasing and unsustainable, calling for more *efficient* developments of modern large-scale machine learning.

Efficient learning involves several aspects, centering around models, data, optimization, systems, and so on (Shen et al. [2023]). For *data-efficient* machine learning, the core is to properly evaluate the importance per data sample in the original (large) datasets. A broad array of methods is applied in a *static* manner, or known as the offline (coreset) selection, where the samples’ importance is determined before the formal training. By leveraging feature representations of data (Swayamdipta et al. [2020]; Xie et al. [2023b]), this importance can be either evaluated based on a variety of metrics such as distances (Huang et al. [2023]; Xia et al. [2023]; Abbas et al. [2023]), uncertainties (Coleman et al. [2020]; Margatina et al. [2021]), errors (Toneva et al. [2019]; Paul et al. [2021]), etc., or learned via procedures from the meta optimization (Killamsetty et al. [2021c,b]; Jain et al. [2024]; Wang et al. [2022]) and dataset distillation (Nguyen et al. [2021]; Wang et al. [2022]; Zhao and Bilen [2023]), or directly assessed by LLMs (Sachdeva et al. [2024]). See more detailed discussions in Appendix A. However, these approaches can be prohibitively expensive to apply in practice, since their potential dependence on feature representations requires additional (pre-)training in advance.

Another array of methods lies in a *dynamic* sense, or known as the online (batch) selection, where the samples’ importance is simultaneously evaluated along the training process. Dynamic sampling methods can be further divided into two categories: *set* level selection, to prune the whole dataset at the beginning of each epoch (Qin et al. [2024]; Raju et al. [2021]; Thao Nguyen et al. [2023]; Attendu and Corbeil [2023]), and *batch* level selection, to sample subsets from original batches for back propagation (Kawaguchi and Lu [2020]; Katharopoulos and Fleuret [2017, 2018]; Mindermann et al. [2022]). Nevertheless, these dynamic sampling methods leverage similar strategies to evaluate the samples’ importance. Based on the naive intuition that samples’ contributions to the learning are directly associated with gradient updates, it is natural to re-weight data samples with scales of gradients or losses during training. Sampling methods based on

*University of California, Berkeley. Email: ziheng_cheng@berkeley.edu

[†]Microsoft Research Asia. Email: lzhong@microsoft.com

[‡]Microsoft Research Asia. Email: jiang.bian@microsoft.com

the gradients (Hanchi et al. [2022]; Wang et al. [2024b]; Gu et al. [2025]; Wang et al. [2025, 2024a]) usually suffer from significant computation and memory loads. Sampling methods based on the loss dynamics can involve current losses (Jiang et al. [2019]; Loshchilov and Hutter [2016]; Qin et al. [2024]; Thao Nguyen et al. [2023]; Kumar et al. [2023]; Balaban et al. [2023]) and historical losses (Attendu and Corbeil [2023]; Raju et al. [2021]; Sagawa et al. [2020]) and also adopt reference models (Mindermann et al. [2022]; Deng et al. [2023]; Xie et al. [2023a]). See more detailed discussions in Appendix A. However, these approaches exploit the information of losses inadequately by only involving “absolute” loss values, without finer considerations on their dynamical “variations” during training.

To tackle these issues, we propose a simple novel dynamic sampling framework, **Evolved Sampling (ES)**. Unlike previous sampling methods, ES determines the importance/weights of data samples based on both (zero-order) losses and additional (first-order) loss *differences* along the training dynamics. By augmenting and balancing these two orders, ES can **flexibly tune the portion of oscillations (high frequencies) presented in loss signals**, and conducts *batch* level selection without the demand of pre-trained reference models. Importantly, ES employs an equivalent dynamical scheme to compute sampling weights *without explicitly storing historical losses*, and *only computations regarding losses are involved to implicitly calculate the required loss differences*, implying the negligible memory costs and mild computation overhead additionally introduced by weight calculations. Due to its simplicity, ES is effortless to implement, while significantly reducing the number of samples used for back propagations (BPs) and consequently saving the overall wall-clock time without degrading the overall performance. Moreover, ES facilitates convenient extensions to data pruning on the *set* level, i.e., **Evolved Sampling with Pruning (ESWP)**, leading to further accelerations with lossless learning performance. We demonstrate the differences in details between our proposed methods (ES/ESWP) and previous dynamic sampling methods in Tab. 1.

Table 1: Comparison of different dynamic sampling methods. The “history” denotes whether the method uses historical (loss) information along the training. The “dif” column stands for whether the method uses dynamical variations of losses during the training. The last column summarizes the ratio of samples used for back propagations (BPs) relative to the standard training. Here, r stands for the pruning ratio for *set* level methods (pruning data samples of the whole epoch), and b/B represents the pruning ratio for *batch* level methods (selecting a mini-batch b (subset) from a meta-batch B).

	<i>set</i>	<i>batch</i>	history	dif	# of samples for BP
UCB (Raju et al. [2021])	✓		✓		$1 - r$
KA (Thao Nguyen et al. [2023])	✓				$1 - r$
InfoBatch (Qin et al. [2024])	✓				$1 - r$
Loss (Katharopoulos and Fleuret [2017])		✓			b/B
Order (Kawaguchi and Lu [2020])		✓			b/B
ES (ours)		✓	✓	✓	b/B
ESWP (ours)	✓	✓	✓	✓	$(1 - r)b/B$

Our contributions can be summarized as follows:

- On the theoretical side, we provide quantitative convergence analysis of the loss re-weighted gradient descent (GD) under idealized settings. Motivated by this, we propose a simple novel dynamic sampling framework ES(WP) that can *implicitly* incorporate (and balance) additional dynamical *differences* of losses *without explicitly storing historical values and calculating variations*. By further injecting higher-order dynamical information, one can flexibly tune the portion of oscillations (high frequencies) presented in loss signals with quantitative guidance.
- On the empirical side, we carry out extensive experiments to verify the effectiveness, efficiency, and flexibility of ES(WP). It is shown that ES(WP) consistently achieves lossless training accelerations across various pre-training and post-training tasks, saving up to 45% training time.

The rest of this paper is organized as follows. In Sec. 2, we provide the motivation of loss-based dynamic sampling methods. In Sec. 3, we present the proposed methods with theoretical justifications and complexity

analysis. Experiments and ablation studies are provided in Sec. 4. The discussions and outlook are provided in Sec. 5. Related works and all the details of proofs and experiments are in the appendices.

Notations. We use normal letters to denote scalars, and boldfaced lower-case letters for vectors. We denote the cardinality of a set S by $|S|$. Let $[n] := \{1, 2, \dots, n\}$ for $n \in \mathbb{N}_+$. Let $\mathbf{1}_n \in \mathbb{R}^n$ be the vector of all ones. $\lceil c \rceil$ represents the smallest positive integer such that $\lceil c \rceil \geq c$. We use the big-O notation $f(t) = O(g(t))$ to represent that f is bounded above by g asymptotically, i.e., there exists a universal $c > 0, t_0 > 0$ such that $f(t) \leq cg(t)$ for any $t \geq t_0$.

2 Preliminaries and Motivations

2.1 Preliminaries

The classic setting of general machine learning tasks is as follows. Given a dataset $\mathcal{D} := \{z_i\}_{i=1}^n$ with $z_i := (x_i, y_i)$ (labeled) or $z_i := x_i$ (unlabeled) of the size $n \in \mathbb{N}_+$, the goal is to solve the empirical risk minimization (ERM) problem: $\min_{\theta \in \Theta} \hat{L}_n(\theta) := \frac{1}{n} \sum_{i=1}^n \ell_i(\theta)$, where $\ell_i(\theta) := \ell(f(x_i; \theta), y_i)$ or $\ell_i(\theta) := \ell(f(x_i; \theta))$. Here, $\ell(\cdot, \cdot)$ or $\ell(\cdot)$ denotes the non-negative loss function, and $\hat{L}_n(\theta)$ represents the empirical averaged loss over n data samples. When n is large, a common routine is to compute stochastic gradient on a random batch instead of the whole training set. For instance, starting from an initialization $\theta(0) = \theta_0$, the SGD optimizer updates model parameters by $\theta(t+1) = \theta(t) - \eta_t \nabla_{\theta} \hat{L}_n(\theta(t)) \approx \theta(t) - \frac{\eta_t}{B} \sum_{j=1}^B \nabla_{\theta} \ell_{i_j}(\theta(t))$, where $\{\eta_t\}_{t \in \mathbb{N}}$ denotes learning rates, and $B \leq n$ is the batch size. The standard sampling method is to draw the batch $\{z_{i_j}\}_{j=1}^B \subset \mathcal{D}$ uniformly without replacement for $\lceil n/B \rceil$ iterations in one epoch, which we refer as the standard batched sampling (baseline, no data selection).

2.2 Theoretical Motivations

Obviously, the standard batched sampling takes equal treatment to data samples. This can be *inefficient* since different samples may have varied importance to the learning task at different training stages: As the training proceeds, there are inevitably samples that are fitted more accurately compared with the others, leading to lower priority to learn these better-fitted samples in the sequel. Hence, it is necessary to assign *adaptive* weights for data samples during training.

Convergence of loss re-weighted GD. As discussed before, it is intuitively reasonable to measure the samples' importance with scales of losses along the training, putting more weights on samples with larger losses. The experiments in [Katharopoulos and Fleuret \[2017\]](#) and [Kawaguchi and Lu \[2020\]](#) have suggested that this kind of "loss-weighted" gradient decent dynamics can accelerate learning in practice compared to vanilla GD (without data re-weighting). To step further, this work develops these former literatures in theory by first mathematically proving the following convergence rate.

Proposition 2.1 (Reduced version; see a full version in Proposition B.1). *Consider the continuous-time idealization of the loss-weighted gradient decent, i.e.*

$$\frac{d}{ds} \hat{\theta}_n^{lw}(s) = - \sum_{i=1}^n \frac{\ell_i(\hat{\theta}_n^{lw}(s))}{\sum_{j=1}^n \ell_j(\hat{\theta}_n^{lw}(s))} \nabla_{\theta} \ell_i(\hat{\theta}_n^{lw}(s)), \quad (2.1)$$

with the initialization $\hat{\theta}_n^{lw}(0) = \theta_0$. Assume that there exists θ^* such that $\hat{L}_n(\theta^*) = 0$ and $\ell_i(\cdot)$ is convex for each $i \in [n]$. Then, we have the more-than sub-linear convergence rate of (Eq. (2.1)):

$$\hat{L}_n(\hat{\theta}_n^{lw}(s_0)) - \hat{L}_n(\theta^*) \leq \frac{1}{2s} \|\theta_0 - \theta^*\|_2^2 - \frac{1}{s} \int_0^s \Delta(s') ds', \quad s > 0, s_0 \in [0, s], \quad (2.2)$$

where $\Delta(\cdot)$ is a positive-valued function on $[0, \infty)$.

Proposition 2.1 suggests that (under certain regularity conditions) the loss-weighted gradient flow converges more than sub-linearly to the global minimum, while the standard gradient flow (i.e. the continuous-time idealization of vanilla GD) only has the sub-linear convergence.¹

To formulate, for any $i \in [n]$ and $t \in \mathbb{N}$, define $w_i(t)$ as the (unnormalized) weight of the i -th sample at the t -th (training) step. For the standard batched sampling, we obviously have the uniform weights: $w_i(t) \equiv 1/n$. For the loss-weighted sampling Eq. (2.1), one calculates the sampling probability as

$$p_i(t) \propto w_i(t) = \ell_i(\boldsymbol{\theta}(t)), \quad (2.3)$$

i.e., the weight is set as the current loss value. On top of that, there are also some variants of loss-weighted sampling strategies: For instance, Kumar et al. [2023] sets $w_i(t) = g(\ell_i(\boldsymbol{\theta}(t)))$, where the function $g(\cdot)$ is pre-defined based on the theory of robust optimization; Kawaguchi and Lu [2020] directly selects top- q samples in terms of current losses per training step, which can be regarded as another realization of Kumar et al. [2023].

3 Methods and Analysis

3.1 Evolved Sampling

In general machine learning tasks, the typical behaviors of averaged losses often appear decent trends overall, but can oscillate meanwhile due to the noises in training dynamics. This introduces the *instability* issue of sampling schemes (e.g. Eq. (2.3)) applied in practice, i.e., the loss-weighted sampling scheme like Eq. (2.3) is intrinsically *sensitive* to possibly large *variations* of (individual) losses and not robust to possible noises. In this regard, it is natural to further incorporate higher-order information in the loss dynamics to derive more stable sampling, such as the first-order derivatives of losses $\frac{d}{dt} \ell_i(\boldsymbol{\theta}(t))$, or the corresponding discretizations (i.e. “differences” of losses) $\ell_i(\boldsymbol{\theta}(t+1)) - \ell_i(\boldsymbol{\theta}(t))$ for any $i \in [n]$ and $t \in \mathbb{N}$. Since this requires additional storage for historical losses per sample, one can *implicitly* achieve the same goal e.g. based on the following proposition.

Proposition 3.1. For any $i \in [n]$ and $t \in \mathbb{N}$, define the sampling probability as

$$\begin{aligned} p_i(t) \propto w_i(t) &= \beta_1 s_i(t-1) + (1 - \beta_1) \ell_i(\boldsymbol{\theta}(t)), \\ s_i(t) &= \beta_2 s_i(t-1) + (1 - \beta_2) \ell_i(\boldsymbol{\theta}(t)) \end{aligned} \quad (3.1)$$

with $s_i(0) = 1/n$, and $\beta_1, \beta_2 \in [0, 1]$ as two hyper-parameters. Then for any $\beta_2 \neq 1$, we have

$$w_i(t) = (1 - \beta_2) \sum_{k=1}^t \beta_2^{t-k} \ell_i(\boldsymbol{\theta}(k)) + (\beta_2 - \beta_1) \underbrace{\sum_{k=1}^{t-1} \beta_2^{t-1-k} (\ell_i(\boldsymbol{\theta}(k+1)) - \ell_i(\boldsymbol{\theta}(k)))}_{\text{losses' dynamical differences}} + O(\beta_2^t). \quad (3.2)$$

The proof is deferred to Appendix B.2. We discuss the implications of Proposition 3.1 as follows:

- The sampling scheme Eq. (3.1) reduces to Eq. (2.3) when setting $\beta_1 = \beta_2 = 0$,² hence it is an extension by augmenting the information of losses’ dynamical differences.
- Proposition 3.1 suggests that one can incorporate additional dynamical variations of losses into the calculation of sampling weights through Eq. (3.1), *without explicitly storing historical losses and calculating differences* (as in Eq. (3.2)), making Eq. (3.1) an efficient sampling scheme by saving both memory and computation compared to Eq. (3.2).
- Based on Eq. (3.2), the strengths of losses and their dynamical differences can be flexibly balanced via the hyper-parameters (β_1, β_2) , leading to improved stability of Eq. (3.1) under oscillatory loss dynamics. This intuition is illustrated in Fig. 1. By setting $(\beta_1, \beta_2) \rightarrow (0^+, 1^-)$, we are able to exploit the long-term

¹Although this sharper convergence bound cannot imply learning accelerations solely in theory, accelerations are often observed in practical simulations (e.g. Table 1, 3 and Figure 3, 4 in Kawaguchi and Lu [2020]).

²Also, it is obvious that Eq. (3.1) reduces to the standard batched sampling when setting $\beta_1 = \beta_2 = 1$.

historical information during training (via β_2), while focusing on the importance of current losses (via β_1) and thus can get the best of both world.³

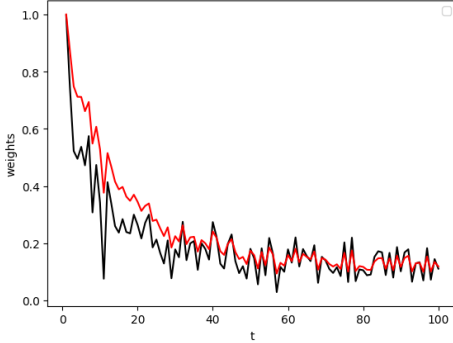


Figure 1: The output weights of different sampling schemes, where the black curve denotes Eq. (2.3), while the red curve represents Eq. (3.1) ($(\beta_1, \beta_2) = (0.5, 0.9)$). Here, we draw the black curve as a decayed function with random perturbations, to mimic typical behaviors of loss curves in general machine learning. It is shown that the sampling scheme Eq. (2.3) is sensitive w.r.t. oscillations. However, when losses oscillate, the sampling scheme Eq. (3.1) reacts moderately by not only reserving some portion of dynamical details of losses (high frequency information), but also remaining necessary robustness by capturing the overall trend (low frequency information), with the flexibility to trade off in between by tuning (β_1, β_2) . See theoretical analysis in Sec. 3.2.

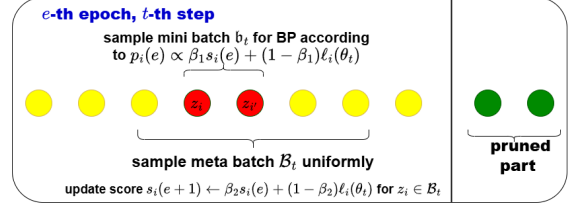


Figure 2: An illustration of ES(WP). At the beginning of the e -th epoch, we optionally randomly prune the whole dataset (“pruning”), according to the probability proportional to the weights $\{w_i(e)\}_{i=1}^n$ defined in Eq. (3.1). At the t -th step, we first sample a meta-batch \mathcal{B}_t uniformly without replacement from the remaining dataset; then we sample a mini-batch b_t from \mathcal{B}_t for BP, according to the sampling probability $p_i(\cdot)$ defined in Eq. (3.1). Note that the scores/weights of samples are updated using the *latest* model parameters. At the first/last few epochs, we optionally use the “annealing” strategy (Qin et al. [2024]), i.e. the standard batched sampling without data selection. See algorithm details in Appendix C.

Intuitions. We explain why augmented (loss) differences should work intuitively. Let $\beta_2 > \beta_1$. Given any data sample z_i , if its total loss variations accumulated up to t are positive (say, $l_i(\cdot)$ always increases), the augmented “difference” term in Eq. (3.2) is positive and hence its sampling weight is increased, which is reasonable since the model continually underfits z_i and should then value z_i more. Conversely, if its loss variations accumulated up to t are negative (say, $l_i(\cdot)$ always decreases), the augmented “difference” term in Eq. (3.2) is negative and hence its sampling weight is decreased, which is also reasonable since the model continually fits z_i well and should then value z_i less. That is, the augmented “difference” term in Eq. (3.2) plays a role of “damping” to stabilize the data re-weighting. More quantitative justifications can be derived via the frequency analysis (see Sec. 3.2).

ES(WP) framework. We refer the scheme Eq. (3.1) as Evolved Sampling (ES), which conducts data selection on batch level. To further incorporate set level selection, we extend ES to prune data at each epoch, leading to Evolved Sampling With Pruning (ESWP) framework as illustrated in Fig. 2. Note that we optionally adopt annealing techniques to enhance performance. For the essential differences between ES(WP) and previous dynamic sampling methods, one can refer to the taxonomy outlined in Tab. 1. As a plug-and-play framework, ES(WP) can be integrated into any optimizers applied to different tasks, while some recently developed sampling methods (Wang et al. [2024a, 2025]) only work for SGD. In practice, the simple and

³In fact, by Eq. (3.1), it is obvious that smaller β_1 and larger β_2 give larger coefficients of the current loss $l_i(\theta(t))$ and historical score $s_i(t-1)$, respectively, hence we are focusing on the importance of both current losses and historical weights by setting $(\beta_1, \beta_2) \rightarrow (0^+, 1^-)$.

elegant design of the sampling scheme Eq. (3.1) turns out to be surprisingly effective, as shown in extensive experiments.

Remark 1. Here, we allow the randomness to keep samples with lower weights in training, which reduces the biases (and possibly inactive samples) compared to directly discarding them.

3.2 Theoretical Benefits of Evolved Sampling via Fourier Analysis

In this section, we provide mathematical justifications for the sampling scheme Eq. (3.1) by characterizing its frequency properties. To achieve this, we first view $\ell(t)(:= \ell(\theta(t)))$, $s(t)$, $w(t)$ defined in the sampling scheme Eq. (3.1) all as signals in time. For ease of notation, we omit the sample index i here. For a signal in time $f(t)$ (with appropriate regularities), we consider the Laplace transform $\mathcal{L}\{f\}(\omega) = \int_0^\infty e^{-\omega t} f(t) dt$, $\omega \in \mathbb{C}$. Then, according to the Fourier analysis, $|\mathcal{L}\{f\}(i\omega_0)|$ represents the magnitude of f 's ω_0 -frequency for $\omega_0 > 0$ ($i^2 = -1$). We have the following result.

Theorem 3.2. Consider a continuous-time idealization of the sampling scheme Eq. (3.1):

$$w(t) = s(t) + \frac{\beta_2 - \beta_1}{1 - \beta_2} s'(t), \quad s'(t) = (1 - \beta_2)(\ell(t) - s(t)), \quad (3.3)$$

with $s(0) = 1/n$, and $\beta_1, \beta_2 \in (0, 1)$ as two hyper-parameters. Then we have

$$\mathcal{L}\{w\}(\omega) = \frac{(\beta_2 - \beta_1)\omega + (1 - \beta_2)}{\omega + (1 - \beta_2)} \mathcal{L}\{\ell\}(\omega) + O(1/n), \quad (3.4)$$

implying that the transfer function $H(\omega) = \frac{(\beta_2 - \beta_1)\omega + (1 - \beta_2)}{\omega + (1 - \beta_2)}$ satisfies

$$|H(i\omega_0)| \leq 1, \quad \lim_{\omega_0 \rightarrow +\infty} |H(i\omega_0)| = |\beta_2 - \beta_1|. \quad (3.5)$$

The proof is provided in Appendix B.3. Based on Thm. 3.2, we conclude that (i) for all frequencies in the loss signal $\ell(t) = \ell(\theta(t))$, the weight signal $w(t)$ calculated by the sampling scheme Eq. (3.1) does not enlarge them, hence is more stable in the frequency domain given oscillations in loss signals; (ii) for high frequencies in the loss signal $\ell(t) = \ell(\theta(t))$, the weight signal $w(t)$ calculated by the sampling scheme Eq. (3.1) reserves a $|\beta_2 - \beta_1|$ -portion, which can be tuned via betas (frequency tuning). This suggests that the sampling scheme Eq. (3.1) can not only stably capture the overall trend (low frequency), but also flexibly tune the portion of details (high frequency) in loss signals.

3.3 Unveiling the Acceleration Effects via Complexity Analysis

Computation efficiency. The primary source of savings comes from the substantial reduction in the effective batch size during BP, compared with standard sampling (no data selection). Although ES(WP) introduces an extra forward pass (FP) on the selected mini-batch (can be *omitted* if selection is performed only at the set level, e.g., ESWP.), the overhead is modest since FP requires much fewer FLOPs than BP. Consequently, the reduction in BP dominates the overall time complexity, leading to a significant acceleration effect, as observed empirically in Sec. 4.1.

Memory efficiency. From Eq. (3.1), the only additional memory cost of ES(WP) is to store the current score/weight value of each sample, which is negligible compared to the memory cost high-dimensional data itself. Moreover, because ES(WP) reduces the effective sample size in BP, it further decreases memory usage (also verified numerically in Sec. 4.1).

More significant benefits under resource constraints. The advantages of ES(WP) become even more significant in low-resource scenarios where GPU memory is limited and gradient accumulation is required, a typical scenario in fine-tuning large models (e.g., LLMs). In this setting, multiple BP passes must be executed before completing a single model update. Suppose the micro-batch size on each GPU is b_{micro} . Then under standard sampling, the number of BP per update step is $\lceil B/b_{\text{micro}} \rceil$. In contrast, ES(WP) requires only $\lceil b/b_{\text{micro}} \rceil$ BP passes. When $b_{\text{micro}} \leq b$, the time spent on BP under standard sampling can be up to B/b times greater than with ES(WP), underscoring the stronger acceleration of our method in memory-constrained training.

3.4 Hyper-Parameters tuning

The primary hyper-parameters are betas in the sampling scheme Eq. (3.1), which are designed to balance dynamical losses and their differences during training. In experiments, we take the default values of (β_1, β_2) , which are obtained by a fine-grained grid search in small-scale simulations (Sec. 4.3). These defaults are consistently validated to be (locally) optimal in small-scale experiments, and their superior effectiveness remain in large-scale tasks (Sec. 4.1, (ii) & (iii), Sec. 4.2).⁴ The other hyper-parameters, including mini-batch sizes, the pruning ratio and annealing epochs, are all responsible for trade-offs between the learning performance and training speed. All of them are user-defined, similar to previous data selection methods such as Qin et al. [2024]; Thao Nguyen et al. [2023]; Raju et al. [2021]. We also perform comprehensive ablations in Sec. 4.3.

4 Experiments

In this section, we provide numerical simulations on the proposed method ES(WP) to demonstrate its superiority in terms of effectiveness, efficiency, robustness and flexibility.

4.1 Effectiveness and Efficiency

We compare the proposed methods ES/ESWP, with a group of former dynamic sampling approaches, including the standard batched sampling (Baseline), Ordered SGD (Order; Kawaguchi and Lu [2020]), Loss (Katharopoulos and Fleuret [2017], i.e., the sampling scheme Eq. (2.3)), InfoBatch (Qin et al. [2024]), KAKURENBO (KA; Thao Nguyen et al. [2023]), UCB (Raju et al. [2021]). For fair comparisons, all these sampling methods are loss-based, hence *much more light-weighted than gradient-based ones*, and *do not require to (pre)-train or exploit additional models*. See Appendix A, Paragraph “Dynamic sampling” for detailed discussions. For all sampling methods, the hyper-parameters used in data pre-processing and optimization follow standard configurations and are maintained the same (see more details in Appendix D). All reported results are evaluated on the average of 3-4 independent random trials..

Configurations. For ES/ESWP, the default hyper-parameters are as follows: In Eq. (3.1), $(\beta_1, \beta_2) = (0.2, 0.9)$ for ES, $(\beta_1, \beta_2) = (0.2, 0.8)$ for ESWP; for both ES and ESWP, the ratio of mini-batch size (b) over meta-batch size (B) is $b/B = 25\%$; if applicable, the annealing ratio is 5%, i.e., no data selection is performed at the first/last 5% epochs; for ESWP, the pruning ratio is 20%. For the two batch level data selection methods (Order, Loss), we apply the same mini/meta-batch size as ES(WP). For InfoBatch, KA and UCB (set level data selection methods), we use the default hyper-parameters in original papers (see more details in Appendix D.7).

Results. We report the test classification accuracy and overall wall-clock time for the evaluation of both effectiveness and efficiency. The results are as follows.

⁴Notably, here we follow a *common routine* of hyper-parameters also adopted in e.g. Qin et al. [2024]; Wang et al. [2024b]; Thao Nguyen et al. [2023], to reuse default hyper-parameters (obtained by grid search in small-scale simulations) in large-scale experiments, without further tuning. This also indicates that the joint effect of betas is robust, and the gain of ES(WP) is not from simply introducing/tuning more hyper-parameters, but essentially from the augmented losses’ differences.

(i) For small-scale tasks, we train ResNet models on CIFAR datasets, and summarize the performance of different sampling methods in Tab. 2. It is shown that the batch level data selection methods (Loss, Order, ES) typically exhibit limited accelerations on these small-scale tasks, since these methods often require additional forward propagation overheads that are not negligible compared to BPs. Nevertheless, ES is the only algorithm that achieves lossless accelerations across all sampling methods. Notably, ESWP saves the most computation time while maintaining the best performance (also comparable to Baseline) among set level data selection methods (UCB, KA, InfoBatch).

Table 2: The test accuracy (%) and saved time of training ResNet models on CIFAR datasets.

	CIFAR-10 (R-18)	CIFAR-100 (R-18)	CIFAR-100 (R-50)
Baseline	95.4	78.8	81.1
UCB (Raju et al. [2021])	95.2 _{±0.2} 18%	77.6 _{±1.2} 18%	80.5 _{±0.6} 24%
KA (Thao Nguyen et al. [2023])	95.3 _{±0.1} 21%	78.1 _{±0.7} 21%	80.2 _{±0.9} 24%
InfoBatch (Qin et al. [2024])	95.3 _{±0.1} 21%	78.4 _{±0.4} 24%	80.4 _{±0.7} 28%
Loss (Katharopoulos and Fleuret [2017])	95.3 _{±0.1} 11%	78.4 _{±0.4} 10%	80.5 _{±0.6} 12%
Order (Kawaguchi and Lu [2020])	95.4 _{±0.0} 11%	78.5 _{±0.3} 10%	80.9 _{±0.2} 12%
ES	95.4 _{±0.0} 10%	78.8 _{±0.0} 10%	81.1 _{±0.0} 11%
ESWP	95.3 _{±0.1} 24%	78.6 _{±0.2} 24%	80.6 _{±0.5} 31%

Table 3: The test accuracy and saved time of fully fine-tuning ViT-Large on ImageNet-1K.

	Time ↓	Acc. (%)
Baseline	–	84.4
UCB	23.6%	84.2 _{±0.2}
KA	25.3%	84.3 _{±0.1}
InfoBatch	23.5%	84.7 _{±0.3}
Loss	36.4%	84.3 _{±0.1}
Order	38.2%	84.2 _{±0.2}
ES	26.0%	84.7 _{±0.3}
ESWP	40.7%	85.0 _{±0.6}

Selected samples by ES(WP). In Appendix D.2, we provide a visualization of selected samples by ES(WP). Following Mindermann et al. [2022], we also plot the test accuracy versus the number of samples used for back propagations (BPs) for Baseline and ES/ESWP in Fig. 10. It is clear that ES/ESWP can significantly reduce the BP calculation costs and thus improve the learning efficiency.

(ii) For large-scale tasks, we fully fine-tune ViT-Large on ImageNet-1K, and summarize the performance in Tab. 3. Under this setting, ES consistently achieves the best performance among batch level data selection methods and the second-to-highest accuracy across all sampling methods. Notably, ESWP attains the highest accuracy and the most significant wall-clock time reduction, suggesting that ESWP inherits the advantages of both set and batch level data selection methods. In addition, it is observed that the training speed-up of batch level methods gets far more significant given these large-scale tasks, conversely surpassing the set level methods compared to (i). This is due to the dominance of the saved computation in BPs. Furthermore, many sampling methods achieve higher accuracies than Baseline, implying the huge potential of data selection in large-scale deep learning. We also numerically evaluate the corresponding overall memory usage of ES (49.7GB) and ESWP (49.1GB), which are also reduced compared to Baseline (52.4GB), verifying the efficiency of ES(WP) in terms of memory loads besides computation costs for large-scale tasks.

(iii) For (large-scale) distributed learning tasks, we pre-train ViT-Large using MAE (He et al. [2022]), and then fine-tune on ImageNet-1K without data selection. We plot the re-construction loss curves in Fig. 3 and report final accuracy after fine-tuning in Tab. 4. It is shown that ESWP achieves lossless acceleration over Baseline, and consistently outperforms the previous SOTA method InfoBatch.

(iv) For NLP tasks, we fully fine-tune ALBERT-Base-v2 on GLUE, and summarize the results in Tab. 5. Across most datasets and on average, ES/ESWP outperforms all the other sampling methods, and shows improved performance over Baseline with significant reduction of computation time.

4.2 Low-Resource Settings: More Acceleration in LLM Fine-tuning

In this section, we investigate the low-resource setting by fine-tuning Qwen2.5-Math-1.5B [Yang et al., 2024] on a single NVIDIA A100 (40GB). We sample 30K instances from NuminaMath CoT [LI et al., 2024], and conduct SFT with a maximum token length 1024 and thus $b_{\text{micro}} = 8$. We set $B = 32, b = 8$ and the pruning ratio as 0.2 for ESWP. The averaged evaluation results on MATH500 [Hendrycks et al., 2021], AIME24, and OlympiadBench [He et al., 2024] are shown in Fig. 4, where we evaluate the model after 1K, 2K, and 4K training

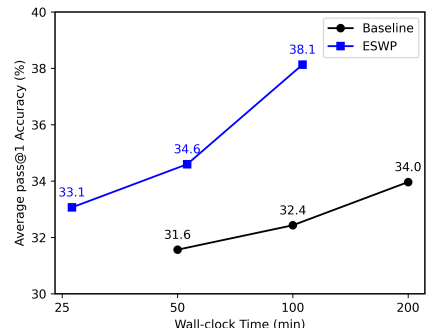


Figure 4: Results of Qwen SFT.

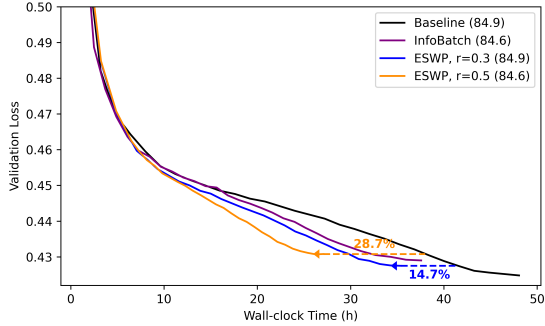


Figure 3: Re-construction losses of MAE-based pre-training of ViT-Large on ImageNet-1K. The number in the bracket in the legend is the validation accuracy (%) after fine-tuning, and r stands for the pruning ratio.

steps. Under this low-resource setting, the time cost of BPs is significant due to gradient accumulations, whereas ESWP can reduce this cost by selecting a much smaller effective mini-batch, thereby achieving learning accelerations. This highlights the superiority of ESWP in computation-constrained and memory-limited environments, where ESWP shows accelerations with improved performance compared to Baseline. More details are provided in Appendix D.6.

4.3 Ablation Studies

Loss differences, annealing and pruning. We numerically test the effectiveness of the most important component adopted in ES(WP), i.e. the augmented dynamical differences of losses. For completeness, we also test the effect of the annealing technique and pruning strategy. Here, we perform ablations on combinations of “Loss” (the sampling scheme Eq. (2.3)), $\beta_1 = \beta_2 = 0$), “NonDif” (corresponding to $\beta_1 = \beta_2$, see Eq. (3.2)), “Dif” (Eq. (3.1)), corresponding to general betas $\beta_1 \neq \beta_2$) and “A” (Annealing). From Tab. 6, it is observed that: (i) Annealing is an effective technique to boost performance; (ii) Although sampling only involving historical losses (“Non-Dif”) can contribute to the improvements, the additional incorporation of dynamical loss differences consistently provides more substantial benefits to the learning process (see consistent non-trivial improvements for various datasets and models in the last two rows of Tab. 6). In Tab. 7, we further ablate for the pruning strategies: Eq. (3.1) used in ESWP versus naive random data pruning. It is shown that both the performance and efficiency of purely random pruning are consistently and substantially worse than ESWP.

From Tab. 6, it is observed that: (i) Annealing is an effective technique to boost performance; (ii) Although sampling only involving historical losses (“Non-Dif”) can contribute to the improvements, the additional incorporation of dynamical loss differences consistently provides more substantial benefits to the learning process (see consistent non-trivial improvements for various datasets and models in the last two rows of Tab. 6). In Tab. 7, we further ablate for the pruning strategies: Eq. (3.1) used in ESWP versus naive random data pruning. It is shown that both the performance and efficiency of purely random pruning are consistently and substantially worse than ESWP.

Table 4: Pre-training time and fine-tuning accuracy.

	Time (h)	Time ↓	Acc. (%)
Baseline	48.1	—	84.9
InfoBatch	37.6	21.8%	84.6 _{↓0.3}
ESWP ($r = 0.3$)	35.1	27.0%	84.9 _{↑0.0}
ESWP ($r = 0.5$)	27.1	44.7%	84.6 _{↓0.3}

Table 5: The validation metric (%) and saved time of fully fine-tuning ALBERT-Base-v2 on GLUE.

	CoLA	SST2	QNLI	QQP	MNLI-m	MRPC	RTE	STSBB	Avg.	Time↓
Baseline	56.7	92.2	91.1	90.3	84.7	88.5	74.0	89.6	83.4	-
InfoBatch	57.9	92.1	91.2	90.3	84.5	89.2	73.8	89.7	83.6 _{↑0.2}	28.3%
Loss	55.1	92.3	91.4	90.2	84.4	88.6	69.6	89.5	82.6 _{↓0.8}	20.8%
Order	55.4	92.6	91.3	90.1	80.9	84.6	63.2	89.4	80.9 _{↓2.5}	20.8%
ES	58.4	92.4	91.4	90.2	84.5	88.7	75.8	89.6	83.9 _{↑0.5}	20.2%
ESWP	57.5	93.1	91.7	90.0	84.7	89.8	72.8	89.4	83.6 _{↑0.2}	33.1%

Table 6: Ablations on the effect of augmented dynamical differences of losses and annealing.

	ResNet-50 CIFAR-100	ALBERT-Base CoLA
Loss	80.5	55.1
Loss + A	80.8	55.8
Loss + NonDif	80.5	57.6
Loss + Dif	81.1	57.5
Loss + A + NonDif	80.4	57.6
ES = Loss + A + Dif	81.1	58.4

Table 7: Ablations on pruning strategies. Here Random denotes purely random data pruning.

	CoLA ALBERT-Base	SST-2 ALBERT-Base
Baseline	55.0, —	91.9, —
Random	53.9 _{↓1.1} , 18%	91.7 _{↓0.2} , 20%
ES	56.2 _{↑1.2} , 16%	92.0 _{↑0.1} , 15%
ESWP	54.7 _{↓0.3} , 24%	92.3 _{↑0.4} , 24%

Trade-offs between performance and speed. We emphasize that batch sizes (b, B), the pruning ratio and annealing epochs in ES(WP) are all user-defined, and flexible to trade off between learning performance and training costs. We evaluate different values of b/B when fine-tuning ViT-Large on ImageNet-1K, and varied pruning ratios when training R-18 on Cifar-100. The results are illustrated in Fig. 5. It is shown that ES robustly achieves lossless acceleration when $b/B \geq 1/16$; when the data selection is too aggressive ($b/B \leq 1/32$), the performance degrades as expected (Fig. 5, left), due to the increase of variances in stochastic gradients. Also, there is a clear trade-off between the performance and speed shown in Fig. 5

(right), where setting the pruning ratio around 20% ~ 30% seems efficient. We further evaluate different annealing ratios (“ar”; i.e., annealing epochs over total epochs) when training R-18 on CIFAR-100 (see Tab. 8), showcasing its robustness.

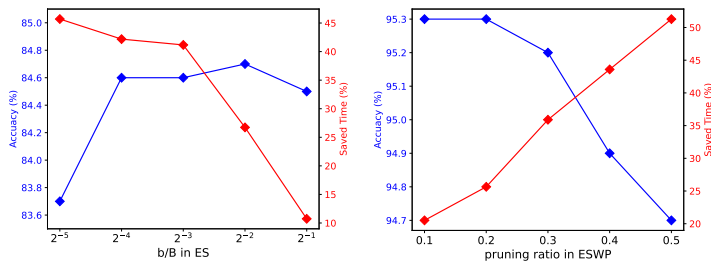


Table 8: Ablations on the annealing (default in bold).

ar	0.0	0.05	0.075	0.1
Acc. (%)	78.60	78.79	78.32	78.20

Figure 5: Trade-offs between learning accuracy and wall-clock time.

Choices of (β_1, β_2) . To investigate the impact of newly introduced hyper-parameters (betas) in ES, we test different choices of (β_1, β_2) when training ResNet-18 on CIFAR datasets and ALBERT-Base model on the CoLA dataset. The results shown in Fig. 6 roughly verify the “optimality” of defaults ($(\beta_1, \beta_2) = (0.2, 0.9)$). In addition, we test denser betas around the defaults when training ResNet-18 on the CIFAR-100 (see Fig. 7), further verifying the (local) optimality of defaults.

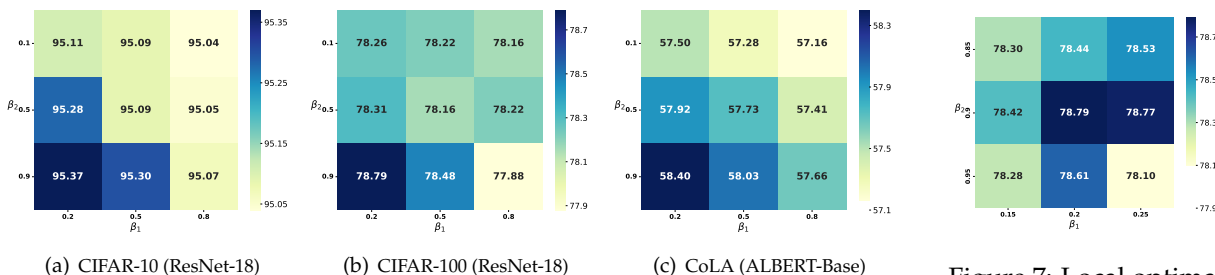


Figure 6: The effect of (β_1, β_2) .

Figure 7: Local optimality of default betas.

5 Conclusion

In this work, we propose a simple yet effective framework, Evolved Sampling, which can be applied to general machine learning tasks to improve the data efficiency in a dynamic manner. By further adopting dynamical differences and flexibly tuning frequencies of historical losses to determine samples’ importance for data selection, Evolved Sampling can achieve lossless training with significant accelerations. Studies in the future may include three aspects: (i) More rigorous mathematical analysis on the effect of data selection (Kolossof et al. [2024]); (ii) More specific applications, such as data selection on domain mixtures (Chen et al. [2023]; Xie et al. [2023a]); (iii) More efficient and scalable implementations, such as data parallelism (You et al. [2017, 2020]). These directions are certainly worthy of explorations in the future.

References

Amro Kamal Mohamed Abbas, Kushal Tirumala, Daniel Simig, Surya Ganguli, and Ari S. Morcos. Semdedup: Data-efficient learning at web-scale through semantic deduplication. In *ICLR 2023 Workshop on Mathematical and Empirical Understanding of Foundation Models*, 2023. URL <https://openreview.net/forum?id=4v1Gm9gv6c>.

- Guillaume Alain, Alex Lamb, Chinnadhurai Sankar, Aaron Courville, and Yoshua Bengio. Variance reduction in SGD by distributed importance sampling. *arXiv preprint arXiv:1511.06481*, 2015.
- Jean-Michel Attendu and Jean-Philippe Corbeil. NLU on data diets: Dynamic data subset selection for NLP classification tasks. In Nafise Sadat Moosavi, Iryna Gurevych, Yufang Hou, Gyuwan Kim, Young Jin Kim, Tal Schuster, and Ameeta Agrawal, editors, *Proceedings of the Fourth Workshop on Simple and Efficient Natural Language Processing (SustaiNLP)*, pages 129–146, Toronto, Canada (Hybrid), July 2023. Association for Computational Linguistics. doi: 10.18653/v1/2023.sustainlp-1.9. URL <https://aclanthology.org/2023.sustainlp-1.9>.
- Olivier Bachem, Mario Lucic, and Andreas Krause. Coresets for nonparametric estimation - the case of DP-Means. In Francis Bach and David Blei, editors, *Proceedings of the 32nd International Conference on Machine Learning*, volume 37 of *Proceedings of Machine Learning Research*, pages 209–217, Lille, France, 07–09 Jul 2015. PMLR. URL <https://proceedings.mlr.press/v37/bachem15.html>.
- Valeriu Balaban, Jayson Sia, and Paul Bogdan. Robust learning under label noise by optimizing the tails of the loss distribution. In *International Conference on Machine Learning and Applications (ICMLA)*, pages 520–527, 2023. doi: 10.1109/ICMLA58977.2023.00078.
- Mayee F. Chen, Nicholas Roberts, Kush Bhatia, Jue Wang, Ce Zhang, Frederic Sala, and Christopher Ré. Skill-it! A data-driven skills framework for understanding and training language models. In A. Oh, T. Naumann, A. Globerson, K. Saenko, M. Hardt, and S. Levine, editors, *Advances in Neural Information Processing Systems*, volume 36, pages 36000–36040. Curran Associates, Inc., 2023. URL https://proceedings.neurips.cc/paper_files/paper/2023/file/70b8505ac79e3e131756f793cd80eb8d-Paper-Conference.pdf.
- Cody Coleman, Christopher Yeh, Stephen Mussmann, Baharan Mirzasoleiman, Peter Bailis, Percy Liang, Jure Leskovec, and Matei Zaharia. Selection via proxy: Efficient data selection for deep learning. In *International Conference on Learning Representations*, 2020. URL <https://openreview.net/forum?id=HJg2b0VYDr>.
- Rudrajit Das, Xi Chen, Bertram Ieong, Parikshit Bansal, and Sujay Sanghavi. Understanding the training speedup from sampling with approximate losses. In Ruslan Salakhutdinov, Zico Kolter, Katherine Heller, Adrian Weller, Nuria Oliver, Jonathan Scarlett, and Felix Berkenkamp, editors, *Proceedings of the 41st International Conference on Machine Learning*, volume 235 of *Proceedings of Machine Learning Research*, pages 10127–10147. PMLR, 21–27 Jul 2024. URL <https://proceedings.mlr.press/v235/das24b.html>.
- Sanjoy Dasgupta, Daniel Hsu, Stefanos Poulis, and Xiaojin Zhu. Teaching a black-box learner. In Kamalika Chaudhuri and Ruslan Salakhutdinov, editors, *Proceedings of the 36th International Conference on Machine Learning*, volume 97 of *Proceedings of Machine Learning Research*, pages 1547–1555. PMLR, 09–15 Jun 2019. URL <https://proceedings.mlr.press/v97/dasgupta19a.html>.
- Zhijie Deng, Peng Cui, and Jun Zhu. Towards accelerated model training via Bayesian data selection. In A. Oh, T. Naumann, A. Globerson, K. Saenko, M. Hardt, and S. Levine, editors, *Advances in Neural Information Processing Systems*, volume 36, pages 8513–8527. Curran Associates, Inc., 2023. URL https://proceedings.neurips.cc/paper_files/paper/2023/file/1af3e0bf5905e33789979f666c31192d-Paper-Conference.pdf.
- Melanie Ducoffe and Frederic Precioso. Adversarial active learning for deep networks: A margin based approach. *arXiv preprint arXiv:1802.09841*, 2018.
- Yuxian Gu, Li Dong, Hongning Wang, Yaru Hao, Qingxiu Dong, Furu Wei, and Minlie Huang. Data selection via optimal control for language models. In *International Conference on Learning Representations*, 2025. URL <https://openreview.net/forum?id=dhAL5fy8wS>.
- Ayoub El Hanchi, David A. Stephens, and Chris J. Maddison. Stochastic reweighted gradient descent. In Kamalika Chaudhuri, Stefanie Jegelka, Le Song, Csaba Szepesvari, Gang Niu, and Sivan Sabato, editors, *Proceedings of the 39th International Conference on Machine Learning*, volume 162 of *Proceedings of Machine Learning Research*, pages 8359–8374. PMLR, 17–23 Jul 2022. URL <https://proceedings.mlr.press/v162/hanchi22a.html>.

- Sariel Har-Peled and Soham Mazumdar. On coresets for k-means and k-median clustering. In *Proceedings of the Thirty-Sixth Annual ACM Symposium on Theory of Computing, STOC '04*, page 291–300, New York, NY, USA, 2004. Association for Computing Machinery. ISBN 1581138520. doi: 10.1145/1007352.1007400. URL <https://doi.org/10.1145/1007352.1007400>.
- Chaoqun He, Renjie Luo, Yuzhuo Bai, Shengding Hu, Zhen Leng Thai, Junhao Shen, Jinyi Hu, Xu Han, Yujie Huang, Yuxiang Zhang, et al. Olympiadbench: A challenging benchmark for promoting agi with olympiad-level bilingual multimodal scientific problems. *arXiv preprint arXiv:2402.14008*, 2024.
- Kaiming He, Xinlei Chen, Saining Xie, Yanghao Li, Piotr Dollár, and Ross Girshick. Masked autoencoders are scalable vision learners. In *Proceedings of the IEEE/CVF conference on computer vision and pattern recognition*, pages 16000–16009, 2022.
- Dan Hendrycks, Collin Burns, Saurav Kadavath, Akul Arora, Steven Basart, Eric Tang, Dawn Song, and Jacob Steinhardt. Measuring mathematical problem solving with the math dataset. *arXiv preprint arXiv:2103.03874*, 2021.
- Lingxiao Huang, Shaofeng H.-C. Jiang, Jianing Lou, and Xuan Wu. Near-optimal coresets for robust clustering. In *International Conference on Learning Representations*, 2023. URL <https://openreview.net/forum?id=Nc1ZkRW8Vde>.
- Nishant Jain, Arun S. Suggala, and Pradeep Shenoy. Improving generalization via meta-learning on hard samples. *arXiv preprint arXiv:2403.12236*, 2024.
- Angela H. Jiang, Daniel L.-K. Wong, Giulio Zhou, David G. Andersen, Jeffrey Dean, Gregory R. Ganger, Gauri Joshi, Michael Kaminsky, Michael Kozuch, Zachary C. Lipton, and Padmanabhan Pillai. Accelerating deep learning by focusing on the biggest losers. *arXiv preprint arXiv:1910.00762*, 2019.
- Angelos Katharopoulos and François Fleuret. Biased importance sampling for deep neural network training. *arXiv preprint arXiv:1706.00043*, 2017.
- Angelos Katharopoulos and Francois Fleuret. Not all samples are created equal: Deep learning with importance sampling. In Jennifer Dy and Andreas Krause, editors, *Proceedings of the 35th International Conference on Machine Learning*, volume 80 of *Proceedings of Machine Learning Research*, pages 2525–2534. PMLR, 10–15 Jul 2018. URL <https://proceedings.mlr.press/v80/katharopoulos18a.html>.
- Kenji Kawaguchi and Haihao Lu. Ordered SGD: A new stochastic optimization framework for empirical risk minimization. In Silvia Chiappa and Roberto Calandra, editors, *Proceedings of the Twenty Third International Conference on Artificial Intelligence and Statistics*, volume 108 of *Proceedings of Machine Learning Research*, pages 669–679. PMLR, 26–28 Aug 2020. URL <https://proceedings.mlr.press/v108/kawaguchi20a.html>.
- Krishnateja Killamsetty, Durga Sivasubramanian, Ganesh Ramakrishnan, Abir De, and Rishabh Iyer. GRAD-MATCH: Gradient matching based data subset selection for efficient deep model training. In Marina Meila and Tong Zhang, editors, *Proceedings of the 38th International Conference on Machine Learning*, volume 139 of *Proceedings of Machine Learning Research*, pages 5464–5474. PMLR, 18–24 Jul 2021a. URL <https://proceedings.mlr.press/v139/killamsetty21a.html>.
- Krishnateja Killamsetty, Durga Sivasubramanian, Ganesh Ramakrishnan, and Rishabh Iyer. GLISTER: Generalization based data subset selection for efficient and robust learning. *Proceedings of the AAAI Conference on Artificial Intelligence*, 35(9):8110–8118, May 2021b. doi: 10.1609/aaai.v35i9.16988. URL <https://ojs.aaai.org/index.php/AAAI/article/view/16988>.
- Krishnateja Killamsetty, Xujiang Zhao, Feng Chen, and Rishabh Iyer. RETRIEVE: Coreset selection for efficient and robust semi-supervised learning. In M. Ranzato, A. Beygelzimer, Y. Dauphin, P. S. Liang, and J. Wortman Vaughan, editors, *Advances in Neural Information Processing Systems*, volume 34, pages 14488–14501. Curran Associates, Inc., 2021c. URL https://proceedings.neurips.cc/paper_files/paper/2021/file/793bc52a941b3951dfdb85fb04f9fd06-Paper.pdf.

- Germain Kolossov, Andrea Montanari, and Pulkit Tandon. Towards a statistical theory of data selection under weak supervision. In *International Conference on Learning Representations*, 2024. URL <https://openreview.net/forum?id=HhfcNgQn6p>.
- Ramnath Kumar, Kushal Majmundar, Dheeraj Nagaraj, and Arun Sai Suggala. Stochastic re-weighted gradient descent via distributionally robust optimization. *arXiv preprint arXiv:2306.09222*, 2023.
- Michael Langberg and Leonard J. Schulman. Universal ϵ -approximators for integrals. In *Proceedings of the Twenty-First Annual ACM-SIAM Symposium on Discrete Algorithms*, SODA '10, page 598–607, USA, 2010. Society for Industrial and Applied Mathematics. ISBN 9780898716986.
- Jia LI, Edward Beeching, Lewis Tunstall, Ben Lipkin, Roman Soletskyi, Shengyi Costa Huang, Kashif Rasul, Longhui Yu, Albert Jiang, Ziju Shen, Zihan Qin, Bin Dong, Li Zhou, Yann Fleureau, Guillaume Lample, and Stanislas Polu. Numinamath. [<https://huggingface.co/AI-MO/NuminaMath-CoT>] (https://github.com/project-numina/aimo-progress-prize/blob/main/report/numina_dataset.pdf), 2024.
- Evan Zheran Liu, Behzad Haghighoo, Annie S. Chen, Aditi Raghunathan, Pang Wei Koh, Shiori Sagawa, Percy Liang, and Chelsea Finn. Just train twice: Improving group robustness without training group information. In Marina Meila and Tong Zhang, editors, *Proceedings of the 38th International Conference on Machine Learning*, volume 139 of *Proceedings of Machine Learning Research*, pages 6781–6792. PMLR, 18–24 Jul 2021. URL <https://proceedings.mlr.press/v139/liu21f.html>.
- Ilya Loshchilov and Frank Hutter. Online batch selection for faster training of neural networks. In *ICLR 2016 Workshop Track*, 2016.
- Katerina Margatina, Giorgos Vernikos, Loïc Barrault, and Nikolaos Aletras. Active learning by acquiring contrastive examples. In Marie-Francine Moens, Xuanjing Huang, Lucia Specia, and Scott Wen-tau Yih, editors, *Proceedings of the 2021 Conference on Empirical Methods in Natural Language Processing*, pages 650–663, Online and Punta Cana, Dominican Republic, November 2021. Association for Computational Linguistics. doi: 10.18653/v1/2021.emnlp-main.51. URL <https://aclanthology.org/2021.emnlp-main.51>.
- Sören Mindermann, Jan Brauner, Muhammed Razzak, Mrinank Sharma, Andreas Kirsch, Winnie Xu, Benedikt Höltingen, Aidan N. Gomez, Adrien Morisot, Sebastian Farquhar, and Yarin Gal. Prioritized training on points that are learnable, worth learning, and not yet learnt. In Kamalika Chaudhuri, Stefanie Jegelka, Le Song, Csaba Szepesvari, Gang Niu, and Sivan Sabato, editors, *Proceedings of the 39th International Conference on Machine Learning*, volume 162 of *Proceedings of Machine Learning Research*, pages 15630–15649. PMLR, 17–23 Jul 2022. URL <https://proceedings.mlr.press/v162/mindermann22a.html>.
- Baharan Mirzasoleiman, Jeff Bilmes, and Jure Leskovec. Coresets for data-efficient training of machine learning models. In Hal Daumé III and Aarti Singh, editors, *Proceedings of the 37th International Conference on Machine Learning*, volume 119 of *Proceedings of Machine Learning Research*, pages 6950–6960. PMLR, 13–18 Jul 2020. URL <https://proceedings.mlr.press/v119/mirzasoleiman20a.html>.
- Alexander Munteanu, Chris Schwiiegelshohn, Christian Sohler, and David Woodruff. On coresets for logistic regression. In S. Bengio, H. Wallach, H. Larochelle, K. Grauman, N. Cesa-Bianchi, and R. Garnett, editors, *Advances in Neural Information Processing Systems*, volume 31, pages 6561–6570. Curran Associates, Inc., 2018. URL https://proceedings.neurips.cc/paper_files/paper/2018/file/63bfd6e8f26d1d3537f4c5038264ef36-Paper.pdf.
- Deanna Needell, Nathan Srebro, and Rachel Ward. Stochastic gradient descent, weighted sampling, and the randomized Kaczmarz algorithm. In Z. Ghahramani, M. Welling, C. Cortes, N. Lawrence, and K.Q. Weinberger, editors, *Advances in Neural Information Processing Systems*, volume 27. Curran Associates, Inc., 2014. URL https://proceedings.neurips.cc/paper_files/paper/2014/file/b3310bba2be31e673a7ded3386994599-Paper.pdf.
- Timothy Nguyen, Roman Novak, Lechao Xiao, and Jaehoon Lee. Dataset distillation with infinitely wide convolutional networks. In M. Ranzato, A. Beygelzimer, Y. Dauphin, P. S. Liang, and J. Wortman Vaughan, editors, *Advances in Neural Information Processing Systems*, volume 34, pages 5186–5198.

- Curran Associates, Inc., 2021. URL https://proceedings.neurips.cc/paper_files/paper/2021/file/299a23a2291e2126b91d54f3601ec162-Paper.pdf.
- Yonatan Oren, Shiori Sagawa, Tatsunori B. Hashimoto, and Percy Liang. Distributionally robust language modeling. In Kentaro Inui, Jing Jiang, Vincent Ng, and Xiaojun Wan, editors, *Proceedings of the 2019 Conference on Empirical Methods in Natural Language Processing and the 9th International Joint Conference on Natural Language Processing (EMNLP-IJCNLP)*, pages 4227–4237, Hong Kong, China, November 2019. Association for Computational Linguistics. doi: 10.18653/v1/D19-1432. URL <https://aclanthology.org/D19-1432>.
- Adam Paszke, Sam Gross, Francisco Massa, Adam Lerer, James Bradbury, Gregory Chanan, Trevor Killeen, Zeming Lin, Natalia Gimelshein, Luca Antiga, Alban Desmaison, Andreas Kopf, Edward Yang, Zachary DeVito, Martin Raison, Alykhan Tejani, Sasank Chilamkurthy, Benoit Steiner, Lu Fang, Junjie Bai, and Soumith Chintala. Pytorch: An imperative style, high-performance deep learning library. In H. Wallach, H. Larochelle, A. Beygelzimer, F. d'Alché-Buc, E. Fox, and R. Garnett, editors, *Advances in Neural Information Processing Systems*, volume 32. Curran Associates, Inc., 2019. URL https://proceedings.neurips.cc/paper_files/paper/2019/file/bdbca288fee7f92f2bfa9f7012727740-Paper.pdf.
- Mansheej Paul, Surya Ganguli, and Gintare Karolina Dziugaite. Deep learning on a data diet: Finding important examples early in training. In M. Ranzato, A. Beygelzimer, Y. Dauphin, P.S. Liang, and J. Wortman Vaughan, editors, *Advances in Neural Information Processing Systems*, volume 34, pages 20596–20607. Curran Associates, Inc., 2021. URL https://proceedings.neurips.cc/paper_files/paper/2021/file/ac56f8fe9eea3e4a365f29f0f1957c55-Paper.pdf.
- Ziheng Qin, Kai Wang, Zangwei Zheng, Jianyang Gu, Xiangyu Peng, Zhaopan Xu, Daquan Zhou, Lei Shang, Baigui Sun, Xuansong Xie, and Yang You. InfoBatch: Lossless training speed up by unbiased dynamic data pruning. In *International Conference on Learning Representations*, 2024. URL <https://openreview.net/forum?id=C61sk5LsK6>.
- Ravi Raju, Kyle Daruwalla, and Mikko Lipasti. Accelerating deep learning with dynamic data pruning. *arXiv preprint arXiv:2111.12621*, 2021.
- Robin Rombach, Andreas Blattmann, Dominik Lorenz, Patrick Esser, and Björn Ommer. High-resolution image synthesis with latent diffusion models. In *Proceedings of the IEEE/CVF Conference on Computer Vision and Pattern Recognition (CVPR)*, pages 10684–10695, June 2022.
- Noveen Sachdeva, Benjamin Coleman, Wang-Cheng Kang, Jianmo Ni, Lichan Hong, Ed H. Chi, James Caverlee, Julian McAuley, and Derek Zhiyuan Cheng. How to train data-efficient LLMs. *arXiv preprint arXiv:2402.09668*, 2024.
- Shiori Sagawa, Pang Wei Koh, Tatsunori B. Hashimoto, and Percy Liang. Distributionally robust neural networks for group shifts: On the importance of regularization for worst-case generalization. In *International Conference on Learning Representations*, 2020. URL <https://openreview.net/forum?id=ryxGuJrFvS>.
- Tom Schaul, John Quan, Ioannis Antonoglou, and David Silver. Prioritized experience replay. In *International Conference on Learning Representations*, 2016.
- Shai Shalev-Shwartz and Yonatan Wexler. Minimizing the maximal loss: How and why. In Maria Florina Balcan and Kilian Q. Weinberger, editors, *Proceedings of the 33rd International Conference on Machine Learning*, volume 48 of *Proceedings of Machine Learning Research*, pages 793–801, New York, USA, 20–22 Jun 2016. PMLR. URL <https://proceedings.mlr.press/v48/shalev-shwartzb16.html>.
- Li Shen, Yan Sun, Zhiyuan Yu, Liang Ding, Xinmei Tian, and Dacheng Tao. On efficient training of large-scale deep learning models: A literature review. *arXiv preprint arXiv:2304.03589*, 2023.
- Abhinav Shrivastava, Abhinav Gupta, and Ross Girshick. Training region-based object detectors with online hard example mining. In *Proceedings of the IEEE Conference on Computer Vision and Pattern Recognition (CVPR)*, June 2016.

- Leslie N Smith and Nicholay Topin. Super-convergence: Very fast training of neural networks using large learning rates. In *Artificial Intelligence and Machine Learning for Multi-Domain Operations Applications*, volume 11006, pages 369–386. SPIE, 2019.
- Ben Sorscher, Robert Geirhos, Shashank Shekhar, Surya Ganguli, and Ari Morcos. Beyond neural scaling laws: beating power law scaling via data pruning. In S. Koyejo, S. Mohamed, A. Agarwal, D. Belgrave, K. Cho, and A. Oh, editors, *Advances in Neural Information Processing Systems*, volume 35, pages 19523–19536. Curran Associates, Inc., 2022. URL https://proceedings.neurips.cc/paper_files/paper/2022/file/7b75da9b61eda40fa35453ee5d077df6-Paper-Conference.pdf.
- Swabha Swayamdipta, Roy Schwartz, Nicholas Lourie, Yizhong Wang, Hannaneh Hajishirzi, Noah A. Smith, and Yejin Choi. Dataset cartography: Mapping and diagnosing datasets with training dynamics. In Bonnie Webber, Trevor Cohn, Yulan He, and Yang Liu, editors, *Proceedings of the 2020 Conference on Empirical Methods in Natural Language Processing (EMNLP)*, pages 9275–9293, Online, November 2020. Association for Computational Linguistics. doi: 10.18653/v1/2020.emnlp-main.746. URL <https://aclanthology.org/2020.emnlp-main.746>.
- Truong Thao Nguyen, Balazs Gerofi, Edgar Josafat Martinez-Noriega, François Trahay, and Mohamed Wahib. KAKURENBO: Adaptively hiding samples in deep neural network training. In A. Oh, T. Naumann, A. Globerson, K. Saenko, M. Hardt, and S. Levine, editors, *Advances in Neural Information Processing Systems*, volume 36, pages 37900–37922. Curran Associates, Inc., 2023. URL https://proceedings.neurips.cc/paper_files/paper/2023/file/7712b1075f5e0eae297702845714098f-Paper-Conference.pdf.
- Mariya Toneva, Alessandro Sordoni, Remi Tachet des Combes, Adam Trischler, Yoshua Bengio, and Geoffrey J. Gordon. An empirical study of example forgetting during deep neural network learning. In *International Conference on Learning Representations*, 2019. URL <https://openreview.net/forum?id=BJLxm30cKm>.
- Hugo Touvron, Thibaut Lavril, Gautier Izacard, Xavier Martinet, Marie-Anne Lachaux, Timothee Lacroix, Baptiste Rozière, Naman Goyal, Eric Hambro, Faisal Azhar, Aurelien Rodriguez, Armand Joulin, Edouard Grave, and Guillaume Lample. LLaMA: Open and efficient foundation language models. *arXiv preprint arXiv:2302.13971*, 2023.
- Jiachen T. Wang, Tong Wu, Dawn Song, Prateek Mittal, and Ruoxi Jia. GREATS: Online selection of high-quality data for LLM training in every iteration. In A. Globerson, L. Mackey, D. Belgrave, A. Fan, U. Paquet, J. Tomczak, and C. Zhang, editors, *Advances in Neural Information Processing Systems*, volume 37, pages 131197–131223. Curran Associates, Inc., 2024a. URL https://proceedings.neurips.cc/paper_files/paper/2024/file/ed165f2ff227cf36c7e3ef88957dadd9-Paper-Conference.pdf.
- Jiachen T. Wang, Dawn Song, James Zou, Prateek Mittal, and Ruoxi Jia. Capturing the temporal dependence of training data influence. In *International Conference on Learning Representations*, 2025. URL <https://openreview.net/forum?id=uHLgDEgiS5>.
- Kai Wang, Bo Zhao, Xiangyu Peng, Zheng Zhu, Shuo Yang, Shuo Wang, Guan Huang, Hakan Bilen, Xinchao Wang, and Yang You. CAFE: Learning to condense dataset by aligning features. In *Proceedings of the IEEE/CVF Conference on Computer Vision and Pattern Recognition (CVPR)*, pages 12196–12205, June 2022.
- Ziteng Wang, Jianfei Chen, and Jun Zhu. Efficient backpropagation with variance controlled adaptive sampling. In *International Conference on Learning Representations*, 2024b. URL <https://openreview.net/forum?id=gEwKAZZmSw>.
- Ross Wightman et al. Pytorch image models, 2019.
- Xiaobo Xia, Jiale Liu, Jun Yu, Xu Shen, Bo Han, and Tongliang Liu. Moderate coreset: A universal method of data selection for real-world data-efficient deep learning. In *International Conference on Learning Representations*, 2023. URL <https://openreview.net/forum?id=7D5EECb0af9>.
- Sang Michael Xie, Hieu Pham, Xuanyi Dong, Nan Du, Hanxiao Liu, Yifeng Lu, Percy Liang, Quoc V. Le, Tengyu Ma, and Adams Wei Yu. DoReMi: Optimizing data mixtures speeds up language

- model pretraining. In A. Oh, T. Naumann, A. Globerson, K. Saenko, M. Hardt, and S. Levine, editors, *Advances in Neural Information Processing Systems*, volume 36, pages 69798–69818. Curran Associates, Inc., 2023a. URL https://proceedings.neurips.cc/paper_files/paper/2023/file/dcba6be91359358c2355cd920da3fcbd-Paper-Conference.pdf.
- Sang Michael Xie, Shibani Santurkar, Tengyu Ma, and Percy Liang. Data selection for language models via importance resampling. In A. Oh, T. Naumann, A. Globerson, K. Saenko, M. Hardt, and S. Levine, editors, *Advances in Neural Information Processing Systems*, volume 36, pages 34201–34227. Curran Associates, Inc., 2023b. URL https://proceedings.neurips.cc/paper_files/paper/2023/file/6b9aa8f418bde2840d5f4ab7a02f663b-Paper-Conference.pdf.
- An Yang, Beichen Zhang, Binyuan Hui, Bofei Gao, Bowen Yu, Chengpeng Li, Dayiheng Liu, Jianhong Tu, Jingren Zhou, Junyang Lin, et al. Qwen2. 5-math technical report: Toward mathematical expert model via self-improvement. *arXiv preprint arXiv:2409.12122*, 2024.
- Yang You, Igor Gitman, and Boris Ginsburg. Large batch training of convolutional networks. *arXiv preprint arXiv:1708.03888*, 2017.
- Yang You, Jing Li, Sashank Reddi, Jonathan Hseu, Sanjiv Kumar, Srinadh Bhojanapalli, Xiaodan Song, James Demmel, Kurt Keutzer, and Cho-Jui Hsieh. Large batch optimization for deep learning: Training BERT in 76 minutes. In *International Conference on Learning Representations*, 2020. URL <https://openreview.net/forum?id=Syx4wnEtvH>.
- Chiyuan Zhang, Samy Bengio, Moritz Hardt, Benjamin Recht, and Oriol Vinyals. Understanding deep learning requires rethinking generalization. In *International Conference on Learning Representations*, 2017. URL <https://openreview.net/forum?id=Sy8gdB9xx>.
- Bo Zhao and Hakan Bilen. Dataset condensation with distribution matching. In *Proceedings of the IEEE/CVF Winter Conference on Applications of Computer Vision (WACV)*, pages 6514–6523, January 2023.
- Peilin Zhao and Tong Zhang. Stochastic optimization with importance sampling for regularized loss minimization. In Francis Bach and David Blei, editors, *Proceedings of the 32nd International Conference on Machine Learning*, volume 37 of *Proceedings of Machine Learning Research*, pages 1–9, Lille, France, 07–09 Jul 2015. PMLR. URL <https://proceedings.mlr.press/v37/zhaoa15.html>.

A Related Work

Static sampling Methods to sampling statically can be based on geometry, uncertainty, error, meta optimization, dataset distillation, etc. With numerous studies on theoretical guarantees (Har-Peled and Mazumdar [2004]; Huang et al. [2023]; Bachem et al. [2015]), the coreset selection is designed to approximate original datasets with smaller (weighted) subsets, typically achieved by clustering in representation spaces (Xia et al. [2023]; Abbas et al. [2023]; Sorscher et al. [2022]). Uncertainty-based methods use probability metrics such as the confidence, entropy (Coleman et al. [2020]) and distances to decision boundaries (Ducoffe and Precioso [2018]; Margatina et al. [2021]; Dasgupta et al. [2019]; Liu et al. [2021]). Sampling methods based on errors assume that training samples with more contributions to errors are more important. Errors are evaluated with metrics such as forgetting events (Toneva et al. [2019]), GRAND & EL2N score (Paul et al. [2021]), and sensitivity (Langberg and Schulman [2010]; Munteanu et al. [2018]). The meta optimization methods apply a bilevel framework to learn the re-weighting. In general, existing studies such as RETRIEVE (Killamsetty et al. [2021c]), GLISTER (Killamsetty et al. [2021b]), MOLERE (Jain et al. [2024]), CAFE (Wang et al. [2022]) and so on, consider the data selection as the outer objective (over selection weights), and the optimization of model parameters on selected subsets as the inner objective. Dataset distillation aims to synthesize an informative but smaller subset from the original (large) dataset. Although there are multiple implementations to reduce the overall loads, such as distributed kernel computation (Nguyen et al. [2021]), category decoupling (Wang et al. [2022]), random modeling (Zhao and Bilen [2023]) and so on, the dataset distillation still requires to optimize over both the model and data, and is hence expensive. A recent work Sachdeva et al. [2024] also

leverages the zero-shot reasoning capability of instruction-tuned large language models (LLMs) to directly assess the quality of data examples. As is discussed before, these static sampling methods require extra training, leading to considerable costs in both computation and memory.

Dynamic sampling Methods to sampling dynamically typically leverage metrics based on losses and gradients along the training process. Loss-adaptive sampling re-weights data points during the training according to current losses (Jiang et al. [2019]; Loshchilov and Hutter [2016]; Schaul et al. [2016]; Kawaguchi and Lu [2020]; Qin et al. [2024]; Thao Nguyen et al. [2023]; Kumar et al. [2023]; Balaban et al. [2023]; Katharopoulos and Fleuret [2017]; Shrivastava et al. [2016]; Das et al. [2024]) and historical losses (Attendu and Corbeil [2023]; Raju et al. [2021]; Oren et al. [2019]; Sagawa et al. [2020]). To name a few, Ordered SGD (Kawaguchi and Lu [2020]) selects top- q samples in terms of the loss ranking per training step. InfoBatch (Qin et al. [2024]) randomly prunes a portion of less informative samples with losses below the average and then re-scales the gradients. KAKURENBO (Thao Nguyen et al. [2023]) combines current losses with the prediction accuracy and confidence to design a sampling framework with moving-back. Kumar et al. [2023] and Balaban et al. [2023] assign weights as functions of current losses based on the robust optimization theory. Attendu and Corbeil [2023] and Raju et al. [2021] use the exponential moving average over past losses for sampling. There are also studies adopting additional reference models, including Mindermann et al. [2022]; Deng et al. [2023]; Xie et al. [2023a] and so on. These methods either use the information of losses inadequately, or require to train or exploit extra architectures. Gradient-based sampling methods involve (i) gradient matching, such as CRAIG (Mirzasoleiman et al. [2020]) and GRAD-MATCH (Killamsetty et al. [2021a]), which approximate the “full” gradients computed on original datasets via the gradients computed on subsets; (ii) gradient adaption, where the sampling probability is basically determined by current scales of gradients (Hanchi et al. [2022]; Katharopoulos and Fleuret [2018]). Obviously, gradient-based sampling methods lead to much more computation and memory overheads than loss-based methods. A recent work Wang et al. [2024b] uses an intricate layer-wise sampling scheme with complex variance control, which develops former literature Zhao and Zhang [2015]; Alain et al. [2015]; Needell et al. [2014] applying importance sampling methods to accelerate the convergence by reducing variances. A very recent work Gu et al. [2025] also leverages the optimal control theory (i.e. Pontryagin’s maximum principle, PMP) to formulate and decide sampling weights, where both the gradient and Hessian are computed and all historical checkpoints are stored. Obviously, these methods usually suffer from significant computation and memory loads, since extra complexities of at least model dimensions are introduced at every training step. Although there are other gradient-based data selection methods (e.g. Wang et al. [2024a]: local approximation-based selection; Wang et al. [2025]: counterfactual-based selection) developing computation reduction techniques such as the ghost inner-product (of gradients) and generalized Gauss-Newton approximation (of Hessians), these methods are not directly extendable to other popular optimizers like Adam.

Set level versus batch level Dynamic sampling methods can be divided into two categories based on the level where data selection is performed: (i) *set* level selection, to prune the whole dataset at the beginning of each epoch (Qin et al. [2024]; Raju et al. [2021]; Thao Nguyen et al. [2023]; Attendu and Corbeil [2023]); (ii) *batch* level selection, to sample subsets from the original batches for back propagations (Kawaguchi and Lu [2020]; Katharopoulos and Fleuret [2017, 2018]; Mindermann et al. [2022]). These two types of methods, facilitating training accelerations from different perspectives, are not mutually exclusive. However, to the best of our knowledge, we are not aware of any algorithms combining both of them.

B Proofs and Supplemental Theory

B.1 Proof of Proposition 2.1

Proposition B.1 (A full version of Proposition 2.1). *Consider the continuous-time idealization of the gradient decent, i.e. the standard gradient flow training dynamics (no data selection)*

$$\frac{d}{dt} \hat{\theta}_n(t) = -\nabla_{\theta} \hat{L}_n(\hat{\theta}_n(t)) = -\frac{1}{n} \sum_{i=1}^n \nabla_{\theta} \ell_i(\hat{\theta}_n(t)), \quad \hat{\theta}_n(0) = \theta_0, \quad (\text{B.1})$$

and its loss-weighted variant

$$\frac{d}{ds} \hat{\boldsymbol{\theta}}_n^{lw}(s) = - \sum_{i=1}^n \frac{\ell_i(\hat{\boldsymbol{\theta}}_n^{lw}(s))}{\sum_{j=1}^n \ell_j(\hat{\boldsymbol{\theta}}_n^{lw}(s))} \nabla_{\boldsymbol{\theta}} \ell_i(\hat{\boldsymbol{\theta}}_n^{lw}(s)), \quad \hat{\boldsymbol{\theta}}_n^{lw}(0) = \boldsymbol{\theta}_0. \quad (\text{B.2})$$

Assume that there exists $\boldsymbol{\theta}^* \in \Theta$ such that $\hat{L}_n(\boldsymbol{\theta}^*) = 0$,⁵ and $\ell_i(\cdot)$ is convex for each $i \in [n]$. Then, we have the more-than sub-linear convergence rate of (Eq. (B.2)):

$$\hat{L}_n(\hat{\boldsymbol{\theta}}_n^{lw}(s_0)) - \hat{L}_n(\boldsymbol{\theta}^*) \leq \frac{1}{2s} \|\boldsymbol{\theta}_0 - \boldsymbol{\theta}^*\|_2^2 - \frac{1}{s} \int_0^s \Delta(s') ds', \quad s > 0, s_0 \in [0, s], \quad (\text{B.3})$$

where $\Delta(\cdot)$ is a positive-valued function on $[0, \infty)$. Moreover, for any $s, t \geq 0$ such that $\hat{L}_n(\hat{\boldsymbol{\theta}}_n(t)) = \hat{L}_n(\hat{\boldsymbol{\theta}}_n^{lw}(s)) \triangleq l \geq 0$,⁶ we have

$$\frac{d}{ds} \|\hat{\boldsymbol{\theta}}_n^{lw}(s) - \boldsymbol{\theta}^*\|_2^2 \leq -2(l + \Delta(s)), \quad (\text{B.4})$$

$$\frac{d}{dt} \|\hat{\boldsymbol{\theta}}_n(t) - \boldsymbol{\theta}^*\|_2^2 \leq -2l. \quad (\text{B.5})$$

Proof. For any $\boldsymbol{\theta} \in \Theta$, we have

$$\begin{aligned} \frac{d}{dt} \|\hat{\boldsymbol{\theta}}_n(t) - \boldsymbol{\theta}\|_2^2 &= 2 \left\langle \hat{\boldsymbol{\theta}}_n(t) - \boldsymbol{\theta}, \frac{d}{dt} \hat{\boldsymbol{\theta}}_n(t) \right\rangle \\ &= \frac{2}{n} \sum_{i=1}^n \langle \boldsymbol{\theta} - \hat{\boldsymbol{\theta}}_n(t), \nabla_{\boldsymbol{\theta}} \ell_i(\hat{\boldsymbol{\theta}}_n(t)) \rangle \\ &\leq \frac{2}{n} \sum_{i=1}^n (\ell_i(\boldsymbol{\theta}) - \ell_i(\hat{\boldsymbol{\theta}}_n(t))), \end{aligned} \quad (\text{B.6})$$

and

$$\begin{aligned} \frac{d}{ds} \|\hat{\boldsymbol{\theta}}_n^{lw}(s) - \boldsymbol{\theta}\|_2^2 &= 2 \left\langle \hat{\boldsymbol{\theta}}_n^{lw}(s) - \boldsymbol{\theta}, \frac{d}{ds} \hat{\boldsymbol{\theta}}_n^{lw}(s) \right\rangle \\ &= 2 \sum_{i=1}^n \frac{\ell_i(\hat{\boldsymbol{\theta}}_n^{lw}(s))}{\sum_{j=1}^n \ell_j(\hat{\boldsymbol{\theta}}_n^{lw}(s))} \left\langle \boldsymbol{\theta} - \hat{\boldsymbol{\theta}}_n^{lw}(s), \nabla_{\boldsymbol{\theta}} \ell_i(\hat{\boldsymbol{\theta}}_n^{lw}(s)) \right\rangle \\ &\leq 2 \sum_{i=1}^n \frac{\ell_i(\hat{\boldsymbol{\theta}}_n^{lw}(s))}{\sum_{j=1}^n \ell_j(\hat{\boldsymbol{\theta}}_n^{lw}(s))} (\ell_i(\boldsymbol{\theta}) - \ell_i(\hat{\boldsymbol{\theta}}_n^{lw}(s))). \end{aligned} \quad (\text{B.7})$$

Note that

$$\begin{aligned} &\sum_{i=1}^n \left[\frac{\ell_i(\hat{\boldsymbol{\theta}}_n^{lw}(s))}{\sum_{j=1}^n \ell_j(\hat{\boldsymbol{\theta}}_n^{lw}(s))} (\ell_i(\boldsymbol{\theta}) - \ell_i(\hat{\boldsymbol{\theta}}_n^{lw}(s))) - \frac{1}{n} (\ell_i(\boldsymbol{\theta}) - \ell_i(\hat{\boldsymbol{\theta}}_n(t))) \right] \\ &= \sum_{i=1}^n \left(\frac{\ell_i(\hat{\boldsymbol{\theta}}_n^{lw}(s))}{\sum_{j=1}^n \ell_j(\hat{\boldsymbol{\theta}}_n^{lw}(s))} - \frac{1}{n} \right) (\ell_i(\boldsymbol{\theta}) - \ell_i(\hat{\boldsymbol{\theta}}_n^{lw}(s))) + \frac{1}{n} \sum_{i=1}^n (\ell_i(\hat{\boldsymbol{\theta}}_n(t)) - \ell_i(\hat{\boldsymbol{\theta}}_n^{lw}(s))) \\ &= \underbrace{- \sum_{i=1}^n \left(\frac{\ell_i(\hat{\boldsymbol{\theta}}_n^{lw}(s))}{\sum_{j=1}^n \ell_j(\hat{\boldsymbol{\theta}}_n^{lw}(s))} - \frac{1}{n} \right) (\ell_i(\hat{\boldsymbol{\theta}}_n^{lw}(s)) - \ell_i(\boldsymbol{\theta}))}_{T_1} + \underbrace{\left(\hat{L}_n(\hat{\boldsymbol{\theta}}_n(t)) - \hat{L}_n(\hat{\boldsymbol{\theta}}_n^{lw}(s)) \right)}_{T_2}, \end{aligned} \quad (\text{B.8})$$

we analyze T_1, T_2 separately.

⁵One can find empirical evidences of this assumption (the optimal training loss can be zero) in e.g. Zhang et al. [2017] (Figure 1 (a)).

⁶For example, at the initialization, $\hat{L}_n(\hat{\boldsymbol{\theta}}_n(0)) = \hat{L}_n(\boldsymbol{\theta}_0) = \hat{L}_n(\hat{\boldsymbol{\theta}}_n^{lw}(0))$.

(i) T_1 : Note that if $\frac{\ell_i(\hat{\boldsymbol{\theta}}_n^{\text{lw}}(s))}{\sum_{j=1}^n \ell_j(\hat{\boldsymbol{\theta}}_n^{\text{lw}}(s))} \leq \frac{1}{n}$ for any $i \in [n]$, we get $\frac{\ell_i(\hat{\boldsymbol{\theta}}_n^{\text{lw}}(s))}{\sum_{j=1}^n \ell_j(\hat{\boldsymbol{\theta}}_n^{\text{lw}}(s))} = \frac{1}{n}$ for any $i \in [n]$, which holds in the zero probability and implies the triviality. Let $I^+ := \left\{ i \in [n] : \frac{\ell_i(\hat{\boldsymbol{\theta}}_n^{\text{lw}}(s))}{\sum_{j=1}^n \ell_j(\hat{\boldsymbol{\theta}}_n^{\text{lw}}(s))} > \frac{1}{n} \right\} \neq \emptyset$, and $i_{\min}^+ := \arg \min_{i \in I^+} \ell_i(\hat{\boldsymbol{\theta}}_n^{\text{lw}}(s))$, and similarly $I^- := \left\{ i \in [n] : \frac{\ell_i(\hat{\boldsymbol{\theta}}_n^{\text{lw}}(s))}{\sum_{j=1}^n \ell_j(\hat{\boldsymbol{\theta}}_n^{\text{lw}}(s))} \leq \frac{1}{n} \right\} \neq \emptyset$, and $i_{\max}^- := \arg \max_{i \in I^-} \ell_i(\hat{\boldsymbol{\theta}}_n^{\text{lw}}(s))$. Obviously, $\ell_{i_{\min}^+}(\hat{\boldsymbol{\theta}}_n^{\text{lw}}(s)) > \frac{1}{n} \sum_{j=1}^n \ell_j(\hat{\boldsymbol{\theta}}_n^{\text{lw}}(s)) \geq \ell_{i_{\max}^-}(\hat{\boldsymbol{\theta}}_n^{\text{lw}}(s))$, hence $\delta(s) := \ell_{i_{\min}^+}(\hat{\boldsymbol{\theta}}_n^{\text{lw}}(s)) - \ell_{i_{\max}^-}(\hat{\boldsymbol{\theta}}_n^{\text{lw}}(s)) > 0$ for any $s \geq 0$. Notice that $\hat{L}_n(\boldsymbol{\theta}^*) = 0 \Leftrightarrow \ell_i(\boldsymbol{\theta}^*) = 0, \forall i \in [n]$, we have

$$\begin{aligned}
T_1|_{\boldsymbol{\theta}=\boldsymbol{\theta}^*} &= \sum_{i \in I^+} \left(\frac{\ell_i(\hat{\boldsymbol{\theta}}_n^{\text{lw}}(s))}{\sum_{j=1}^n \ell_j(\hat{\boldsymbol{\theta}}_n^{\text{lw}}(s))} - \frac{1}{n} \right) (\ell_i(\hat{\boldsymbol{\theta}}_n^{\text{lw}}(s)) - \ell_i(\boldsymbol{\theta}^*)) \\
&\quad + \sum_{i \in I^-} \left(\frac{\ell_i(\hat{\boldsymbol{\theta}}_n^{\text{lw}}(s))}{\sum_{j=1}^n \ell_j(\hat{\boldsymbol{\theta}}_n^{\text{lw}}(s))} - \frac{1}{n} \right) (\ell_i(\hat{\boldsymbol{\theta}}_n^{\text{lw}}(s)) - \ell_i(\boldsymbol{\theta}^*)) \\
&= \sum_{i \in I^+} \left(\frac{\ell_i(\hat{\boldsymbol{\theta}}_n^{\text{lw}}(s))}{\sum_{j=1}^n \ell_j(\hat{\boldsymbol{\theta}}_n^{\text{lw}}(s))} - \frac{1}{n} \right) \ell_i(\hat{\boldsymbol{\theta}}_n^{\text{lw}}(s)) + \sum_{i \in I^-} \left(\frac{\ell_i(\hat{\boldsymbol{\theta}}_n^{\text{lw}}(s))}{\sum_{j=1}^n \ell_j(\hat{\boldsymbol{\theta}}_n^{\text{lw}}(s))} - \frac{1}{n} \right) \ell_i(\hat{\boldsymbol{\theta}}_n^{\text{lw}}(s)) \\
&\geq \sum_{i \in I^+} \left(\frac{\ell_i(\hat{\boldsymbol{\theta}}_n^{\text{lw}}(s))}{\sum_{j=1}^n \ell_j(\hat{\boldsymbol{\theta}}_n^{\text{lw}}(s))} - \frac{1}{n} \right) \ell_{i_{\min}^+}(\hat{\boldsymbol{\theta}}_n^{\text{lw}}(s)) + \sum_{i \in I^-} \left(\frac{\ell_i(\hat{\boldsymbol{\theta}}_n^{\text{lw}}(s))}{\sum_{j=1}^n \ell_j(\hat{\boldsymbol{\theta}}_n^{\text{lw}}(s))} - \frac{1}{n} \right) \ell_{i_{\max}^-}(\hat{\boldsymbol{\theta}}_n^{\text{lw}}(s)) \\
&= \sum_{i \in I^+} \left(\frac{\ell_i(\hat{\boldsymbol{\theta}}_n^{\text{lw}}(s))}{\sum_{j=1}^n \ell_j(\hat{\boldsymbol{\theta}}_n^{\text{lw}}(s))} - \frac{1}{n} \right) (\ell_{i_{\max}^-}(\hat{\boldsymbol{\theta}}_n^{\text{lw}}(s)) + \delta(s)) + \sum_{i \in I^-} \left(\frac{\ell_i(\hat{\boldsymbol{\theta}}_n^{\text{lw}}(s))}{\sum_{j=1}^n \ell_j(\hat{\boldsymbol{\theta}}_n^{\text{lw}}(s))} - \frac{1}{n} \right) \ell_{i_{\max}^-}(\hat{\boldsymbol{\theta}}_n^{\text{lw}}(s)) \\
&= \ell_{i_{\max}^-}(\hat{\boldsymbol{\theta}}_n^{\text{lw}}(s)) \sum_{i=1}^n \left(\frac{\ell_i(\hat{\boldsymbol{\theta}}_n^{\text{lw}}(s))}{\sum_{j=1}^n \ell_j(\hat{\boldsymbol{\theta}}_n^{\text{lw}}(s))} - \frac{1}{n} \right) + \delta(s) \sum_{i \in I^+} \left(\frac{\ell_i(\hat{\boldsymbol{\theta}}_n^{\text{lw}}(s))}{\sum_{j=1}^n \ell_j(\hat{\boldsymbol{\theta}}_n^{\text{lw}}(s))} - \frac{1}{n} \right) \\
&= \ell_{i_{\max}^-}(\hat{\boldsymbol{\theta}}_n^{\text{lw}}(s))(1-1) + \Delta(s) = \Delta(s), \tag{B.9}
\end{aligned}$$

where $\Delta(s) := \delta(s) \sum_{i \in I^+} \left(\frac{\ell_i(\hat{\boldsymbol{\theta}}_n^{\text{lw}}(s))}{\sum_{j=1}^n \ell_j(\hat{\boldsymbol{\theta}}_n^{\text{lw}}(s))} - \frac{1}{n} \right) > 0$ for any $s \geq 0$. By continuity, $T_1|_{\boldsymbol{\theta}} \geq \Delta(s)/2 > 0$ also holds for any $\boldsymbol{\theta} \approx \boldsymbol{\theta}^*$.

(ii) T_2 : It measures the difference between losses under the standard and loss-weighted gradient flow. Combining (Eq. (B.7)), (Eq. (B.8)) with (Eq. (B.9)) yields that

$$\begin{aligned}
\frac{d}{ds} \|\hat{\boldsymbol{\theta}}_n^{\text{lw}}(s) - \boldsymbol{\theta}^*\|_2^2 &\leq 2 \left[\frac{1}{n} \sum_{i=1}^n (\ell_i(\boldsymbol{\theta}^*) - \ell_i(\hat{\boldsymbol{\theta}}_n(t))) - T_1|_{\boldsymbol{\theta}=\boldsymbol{\theta}^*} + T_2 \right] \\
&\leq 2 \left[(\hat{L}_n(\boldsymbol{\theta}^*) - \hat{L}_n(\hat{\boldsymbol{\theta}}_n(t))) - \Delta(s) + (\hat{L}_n(\hat{\boldsymbol{\theta}}_n(t)) - \hat{L}_n(\hat{\boldsymbol{\theta}}_n^{\text{lw}}(s))) \right] \\
&= 2 \left[(\hat{L}_n(\boldsymbol{\theta}^*) - \hat{L}_n(\hat{\boldsymbol{\theta}}_n^{\text{lw}}(s))) - \Delta(s) \right], \tag{B.10}
\end{aligned}$$

which gives

$$\begin{aligned}
\hat{L}_n(\hat{\boldsymbol{\theta}}_n^{\text{lw}}(s)) - \hat{L}_n(\boldsymbol{\theta}^*) &\leq -\frac{1}{2} \frac{d}{ds} \|\hat{\boldsymbol{\theta}}_n^{\text{lw}}(s) - \boldsymbol{\theta}^*\|_2^2 - \Delta(s) \tag{B.11} \\
\Rightarrow \int_{s_1}^{s_2} \hat{L}_n(\hat{\boldsymbol{\theta}}_n^{\text{lw}}(s)) ds - (s_2 - s_1) \cdot \hat{L}_n(\boldsymbol{\theta}^*) &\leq -\frac{1}{2} \left(\|\hat{\boldsymbol{\theta}}_n^{\text{lw}}(s_2) - \boldsymbol{\theta}^*\|_2^2 - \|\hat{\boldsymbol{\theta}}_n^{\text{lw}}(s_1) - \boldsymbol{\theta}^*\|_2^2 \right) - \int_{s_1}^{s_2} \Delta(s) ds \\
&\leq \frac{1}{2} \|\hat{\boldsymbol{\theta}}_n^{\text{lw}}(s_1) - \boldsymbol{\theta}^*\|_2^2 - \int_{s_1}^{s_2} \Delta(s) ds \tag{B.12}
\end{aligned}$$

for any $s_2 > s_1 \geq 0$. That is

$$\frac{1}{s_2 - s_1} \int_{s_1}^{s_2} \hat{L}_n(\hat{\boldsymbol{\theta}}_n^{\text{lw}}(s)) ds - \hat{L}_n(\boldsymbol{\theta}^*) \leq \frac{1}{2(s_2 - s_1)} \|\hat{\boldsymbol{\theta}}_n^{\text{lw}}(s_1) - \boldsymbol{\theta}^*\|_2^2 - \frac{1}{s_2 - s_1} \int_{s_1}^{s_2} \Delta(s) ds,$$

or for any $s > 0$,

$$\begin{aligned} \frac{1}{s} \int_0^s \hat{L}_n(\hat{\boldsymbol{\theta}}_n^{\text{lw}}(s')) ds' - \hat{L}_n(\boldsymbol{\theta}^*) &\leq \frac{1}{2s} \|\boldsymbol{\theta}_0 - \boldsymbol{\theta}^*\|_2^2 - \frac{1}{s} \int_0^s \Delta(s') ds' \\ &< \frac{1}{2s} \|\boldsymbol{\theta}_0 - \boldsymbol{\theta}^*\|_2^2, \end{aligned} \quad (\text{B.13})$$

which proves (Eq. (B.3)) by further applying the convexity of $\hat{L}_n(\cdot)$ ⁷. Recall that (Eq. (B.6)) can be rewritten as

$$\frac{d}{dt} \|\hat{\boldsymbol{\theta}}_n(t) - \boldsymbol{\theta}^*\|_2^2 \leq 2 (\hat{L}_n(\boldsymbol{\theta}^*) - \hat{L}_n(\hat{\boldsymbol{\theta}}_n(t))). \quad (\text{B.14})$$

Compared with (Eq. (B.10)), for any $s, t \geq 0$ such that $\hat{L}_n(\hat{\boldsymbol{\theta}}_n(t)) = \hat{L}_n(\hat{\boldsymbol{\theta}}_n^{\text{lw}}(s))$, we have (Eq. (B.10))'s RHS < (Eq. (B.14))'s RHS = $-2\hat{L}_n(\hat{\boldsymbol{\theta}}_n(t)) \leq 0$, which implies a sharper convergence bound of the loss-weighted gradient flow (at the same loss level with the standard gradient flow). The proof is completed. \square

Proposition Thm. B.1 suggests that, under certain regularity conditions, the loss-weighted gradient flow converges more than sub-linearly to the global minimum, while the standard gradient flow (i.e the continuous-time idealization of vanilla GD) only has the sub-linear convergence. In addition, at the same loss level, the convergence bound of loss-weighted gradient flow is sharper than that of standard gradient flow. This theoretical characterization, together with practical simulations (e.g., Table 1, 3 and Figure 3, 4 in Kawaguchi and Lu [2020]), fundamentally gives chances to potential learning accelerations by leveraging the loss information in the gradient-based training dynamics.

B.2 Proof of Proposition 3.1

Proof. Define $\boldsymbol{w}(t) := [w_i(t)]_{i \in [n]}$, $\boldsymbol{s}(t) := [s_i(t)]_{i \in [n]}$, and $\boldsymbol{l}(t) := [\ell_i(\boldsymbol{\theta}(t))]_{i \in [n]}$ for any $t \in \mathbb{N}$. The sampling scheme (Eq. (3.1)) can be rewritten as

$$\begin{aligned} \boldsymbol{w}(t) &= \beta_1 \boldsymbol{s}(t-1) + (1 - \beta_1) \boldsymbol{l}(t), \\ \boldsymbol{s}(t) &= \beta_2 \boldsymbol{s}(t-1) + (1 - \beta_2) \boldsymbol{l}(t), \quad \boldsymbol{s}(0) = \mathbf{1}/n. \end{aligned} \quad (\text{B.15})$$

In (Eq. (B.15)), let the first equation minus the second, we get

$$\boldsymbol{w}(t) - \boldsymbol{s}(t) = (\beta_2 - \beta_1) (\boldsymbol{l}(t) - \boldsymbol{s}(t-1)). \quad (\text{B.16})$$

The second equation gives

$$\boldsymbol{s}(t) - \boldsymbol{s}(t-1) = (1 - \beta_2) (\boldsymbol{l}(t) - \boldsymbol{s}(t-1)). \quad (\text{B.17})$$

Combining (Eq. (B.16)) with (Eq. (B.17)), we have

$$\boldsymbol{w}(t) = \boldsymbol{s}(t) + \frac{\beta_2 - \beta_1}{1 - \beta_2} (\boldsymbol{s}(t) - \boldsymbol{s}(t-1)), \quad (\text{B.18})$$

which proves the first equality.

Expanding the second equation, by induction we get

$$\boldsymbol{s}(t) = \beta_2^t \boldsymbol{s}(0) + (1 - \beta_2) \sum_{k=1}^t \beta_2^{t-k} \boldsymbol{l}(k), \quad (\text{B.19})$$

hence

$$\boldsymbol{s}(t) - \boldsymbol{s}(t-1) = \beta_2^{t-1} (\beta_2 - 1) \boldsymbol{s}(0) + (1 - \beta_2) \left[\sum_{k=1}^t \beta_2^{t-k} \boldsymbol{l}(k) - \sum_{k=1}^{t-1} \beta_2^{t-1-k} \boldsymbol{l}(k) \right]$$

⁷That is, by Jensen's inequality, we have $\frac{1}{s} \int_0^s \hat{L}_n(\hat{\boldsymbol{\theta}}_n^{\text{lw}}(s')) ds' \geq \hat{L}_n(\frac{1}{s} \int_0^s \hat{\boldsymbol{\theta}}_n^{\text{lw}}(s') ds')$, and there exists $s_0 \in [0, s]$ such that $\hat{\boldsymbol{\theta}}_n^{\text{lw}}(s_0) = \frac{1}{s} \int_0^s \hat{\boldsymbol{\theta}}_n^{\text{lw}}(s') ds'$.

$$\begin{aligned}
&= -(1 - \beta_2)\beta_2^{t-1}s(0) + (1 - \beta_2) \left[\beta_2^{t-1}\mathbf{l}(1) + \sum_{k=2}^t \beta_2^{t-k}\mathbf{l}(k) - \sum_{k=1}^{t-1} \beta_2^{t-1-k}\mathbf{l}(k) \right] \\
&= -(1 - \beta_2)\beta_2^{t-1}s(0) + (1 - \beta_2) \left[\beta_2^{t-1}\mathbf{l}(1) + \sum_{k=1}^{t-1} \beta_2^{t-1-k}(\mathbf{l}(k+1) - \mathbf{l}(k)) \right] \\
&\approx (1 - \beta_2) \sum_{k=1}^{t-1} \beta_2^{t-1-k}(\mathbf{l}(k+1) - \mathbf{l}(k)) \tag{B.20}
\end{aligned}$$

for relatively large t , and the approximation error is exponentially small (due to $\lim_{t \rightarrow +\infty} \beta_2^t = 0$ for any $\beta_2 \in (0, 1)$). Combining (Eq. (B.18)), (Eq. (B.19)) and (Eq. (B.20)) yields (Eq. (3.2)), and the proof is completed. \square

B.3 Proof of Theorem 3.2

Proof. Consider a continuous-time idealization of the sampling scheme Eq. (3.1):

$$s(t) = \beta_2 s(t-1) + (1 - \beta_2)\ell(t) \Rightarrow s(t) - s(t-1) = (1 - \beta_2)(\ell(t) - s(t-1)) \tag{B.21}$$

$$\Rightarrow s'(t) = (1 - \beta_2)(\ell(t) - s(t)), \tag{B.22}$$

with $\ell(t) := \ell(\theta(t))$, and $\beta_2 \neq 0$. Similarly,

$$\begin{aligned}
w(t) &= \beta_1 s(t-1) + (1 - \beta_1)\ell(t) \Rightarrow w(t) - s(t) = (\beta_2 - \beta_1)(\ell(t) - s(t-1)) \\
&\Rightarrow w(t) = s(t) + (\beta_2 - \beta_1) \frac{s(t) - s(t-1)}{1 - \beta_2} \quad (\text{by (Eq. (B.21))}) \\
&\Rightarrow w(t) = s(t) + \frac{\beta_2 - \beta_1}{1 - \beta_2} s'(t) \\
&\Rightarrow w(t) = (\beta_2 - \beta_1)\ell(t) + (1 - \beta_2 + \beta_1)s(t). \quad (\text{by (Eq. (B.22))}) \tag{B.23}
\end{aligned}$$

Since $\mathcal{L}\{\cdot\}$ is linear and satisfies $\mathcal{L}\{f'\}(\omega) = \omega\mathcal{L}\{f\}(\omega) - f(0)$, we have

$$\begin{aligned}
(\text{Eq. (B.22)}) &\Rightarrow \mathcal{L}\{s'\}(\omega) = (1 - \beta_2)(\mathcal{L}\{\ell\}(\omega) - \mathcal{L}\{s\}(\omega)) = \omega\mathcal{L}\{s\}(\omega) - s(0) \\
&\Rightarrow \mathcal{L}\{s\}(\omega) = \frac{1 - \beta_2}{\omega + (1 - \beta_2)} \mathcal{L}\{\ell\}(\omega) + \frac{s(0)}{\omega + (1 - \beta_2)}, \tag{B.24}
\end{aligned}$$

and

$$\begin{aligned}
(\text{Eq. (B.23)}) &\Rightarrow \mathcal{L}\{w\}(\omega) = (\beta_2 - \beta_1)\mathcal{L}\{\ell\}(\omega) + (1 - \beta_2 + \beta_1)\mathcal{L}\{s\}(\omega) \\
&= \frac{(\beta_2 - \beta_1)\omega + (1 - \beta_2)}{\omega + (1 - \beta_2)} \mathcal{L}\{\ell\}(\omega) + \frac{(1 - \beta_2 + \beta_1)}{\omega + (1 - \beta_2)} s(0), \quad (\text{by (Eq. (B.24))}) \tag{B.25}
\end{aligned}$$

$$\begin{aligned}
&= \frac{(\beta_2 - \beta_1)\omega + (1 - \beta_2)}{\omega + (1 - \beta_2)} \mathcal{L}\{\ell\}(\omega) + \mathcal{L}\{(1 - \beta_2 + \beta_1)s(0) \cdot e^{-(1-\beta_2)t}\}(\omega) \\
&= \frac{(\beta_2 - \beta_1)\omega + (1 - \beta_2)}{\omega + (1 - \beta_2)} \mathcal{L}\{\ell\}(\omega) + O(1/n). \quad (\text{recall } s(0) = 1/n) \tag{B.26}
\end{aligned}$$

Then, the transfer function is $H(\omega) = \frac{(\beta_2 - \beta_1)\omega + (1 - \beta_2)}{\omega + (1 - \beta_2)}$, with

$$|H(i\omega_0)| = \left| \frac{(\beta_2 - \beta_1)i\omega_0 + (1 - \beta_2)}{i\omega_0 + (1 - \beta_2)} \right| = \sqrt{\frac{(\beta_2 - \beta_1)^2 \omega_0^2 + (1 - \beta_2)^2}{\omega_0^2 + (1 - \beta_2)^2}}, \tag{B.27}$$

and

$$|H(i\omega_0)| \leq 1, \quad \lim_{\omega_0 \rightarrow +\infty} |H(i\omega_0)| = |\beta_2 - \beta_1|. \tag{B.28}$$

The proof is completed. \square

B.4 ES to Solve a DRO Problem

From another perspective, ES can be also reformulated as a solution to a distributionally robust optimization (DRO) problem, or more specifically the minimax optimization problem

$$\min_{\boldsymbol{\theta} \in \Theta} \max_{\mathbf{p} \in \Delta^n} L_n(\boldsymbol{\theta}; \mathbf{p}) := \sum_{i=1}^n p_i (\ell_i(\boldsymbol{\theta}) - \ell_i^{\text{ref}}), \quad (\text{B.29})$$

where Δ^n denotes the $(n-1)$ -dimensional probability simplex. This objective leads to a stronger requirement for robust performances on both typical and rare samples compared to the regular ERM (Shalev-Shwartz and Wexler [2016]). Different from traditional DRO, Eq. (B.29) introduces a reference loss ℓ_i^{ref} , with the excess loss $\ell_i(\boldsymbol{\theta}) - \ell_i^{\text{ref}}$ measuring the improvement of the model on the i -th sample with respect to a reference model (typically *pre-trained*; see e.g. Oren et al. [2019]; Xie et al. [2023a]; Mindermann et al. [2022]). The second advantage of ES is to naturally leverage losses of historical models along the training dynamics as a proxy of the reference loss ℓ_i^{ref} in Eq. (B.29), which can be continuously updated without explicitly (pre-)training additional models.

Specifically, we have the following proposition.

Proposition B.2. *Consider to solve the minimax objective Eq. (B.29) via gradient ascent-descent*

$$\begin{cases} \mathbf{p}(t) \propto \mathbf{w}(t) := \mathbf{w}(t-1) + (1-\beta_1)(\ell(\boldsymbol{\theta}(t)) - \ell^{\text{ref}}(\boldsymbol{\theta}(1:t-1))), \\ \boldsymbol{\theta}(t+1) := \boldsymbol{\theta}(t) - \eta_t^\theta \sum_{i=1}^n p_i(t) \nabla_{\boldsymbol{\theta}} \ell_i(\boldsymbol{\theta}(t)), \end{cases} \quad (\text{B.30})$$

where the reference loss is defined as $\ell^{\text{ref}}(\boldsymbol{\theta}(1:t)) := [\ell_i^{\text{ref}}(\boldsymbol{\theta}(1:t))]_{i \in [n]}$ with $\ell_i^{\text{ref}}(\boldsymbol{\theta}(1:t)) := \frac{1-2\beta_1+\beta_1\beta_2}{1-\beta_1} \ell_i(\boldsymbol{\theta}(t)) + \frac{\beta_1(1-\beta_2)^2}{1-\beta_1} \sum_{k=1}^{t-1} \beta_2^{t-1-k} \ell_i(\boldsymbol{\theta}(k)) + \frac{\beta_1(1-\beta_2)\beta_2^{t-1}}{n(1-\beta_1)}$, $i \in [n]$. Then, the dynamics Eq. (B.30) is consistent with gradient descent sampled with the sampling scheme Eq. (3.1).

Proof. The problem (Eq. (B.29)) can be solved in an alternative gradient descent-ascent manner:

$$\begin{aligned} \boldsymbol{\theta}(t+1) &= \boldsymbol{\theta}(t) - \eta_t^\theta \sum_{i=1}^n p_i(t) \nabla_{\boldsymbol{\theta}} \ell_i(\boldsymbol{\theta}(t)), \\ w_i(t+1) &= w_i(t) + \eta_t^w (\ell_i(\boldsymbol{\theta}(t+1)) - \ell_i^{\text{ref}}), \quad p_i(t) = \frac{w_i(t)}{\sum_j w_j(t)}. \end{aligned} \quad (\text{B.31})$$

The sampling scheme (Eq. (3.1)) updates the weights as

$$w_i(t+1) = w_i(t) + (1-\beta_1)(\ell_i(\boldsymbol{\theta}(t+1)) - \ell_i(\boldsymbol{\theta}(t))) + \beta_1(s_i(t) - s_i(t-1)). \quad (\text{B.32})$$

By (Eq. (B.19)), we get

$$s_i(t) - s_i(t-1) = -(1-\beta_2)\beta_2^{t-1}s_i(0) - (1-\beta_2)^2 \sum_{k=1}^{t-1} \beta_2^{t-1-k} \ell_i(\boldsymbol{\theta}(k)) + (1-\beta_2)\ell_i(\boldsymbol{\theta}(t)),$$

hence

$$\begin{aligned} w_i(t+1) &= w_i(t) + (1-\beta_1)(\ell_i(\boldsymbol{\theta}(t+1)) - \ell_i(\boldsymbol{\theta}(t))) - \beta_1(1-\beta_2)\beta_2^{t-1}s_i(0) \\ &\quad - \beta_1(1-\beta_2)^2 \sum_{k=1}^{t-1} \beta_2^{t-1-k} \ell_i(\boldsymbol{\theta}(k)) + \beta_1(1-\beta_2)\ell_i(\boldsymbol{\theta}(t)). \end{aligned} \quad (\text{B.33})$$

Let

$$\ell_i^{\text{ref}} = \frac{1-2\beta_1+\beta_1\beta_2}{1-\beta_1} \ell_i(\boldsymbol{\theta}(t)) + \frac{\beta_1(1-\beta_2)^2}{1-\beta_1} \sum_{k=1}^{t-1} \beta_2^{t-1-k} \ell_i(\boldsymbol{\theta}(k)) + \frac{\beta_1(1-\beta_2)\beta_2^{t-1}}{1-\beta_1} s_i(0), \quad (\text{B.34})$$

then we have

$$w_i(t+1) = w_i(t) + (1-\beta_1)(\ell_i(\boldsymbol{\theta}(t+1)) - \ell_i^{\text{ref}}), \quad (\text{B.35})$$

which coincides with the update formula Eq. (B.31) with $\eta_t^w = 1-\beta_1$. The proof is completed. \square

C More Details of Algorithms

This section presents more details of the ES(WP) sampling framework.

Annealing (optional) Notably, similar to the loss-weighted sampling scheme (Eq. (2.3)) and its further variants, the sampling scheme (Eq. (3.1)) also assigns different weights on the respective gradient of data samples, leading to a biased estimation on the true gradient $\nabla_{\theta} \hat{L}_n(\cdot)$ (with uniform individual weights). Inspired by Qin et al. [2024], we adopt the *annealing* strategy, to perform normal training (with the standard batched sampling, no data selection) at the last few epochs. Besides, to get better initializations of the weights $\{w_i(\cdot)\}_{i \in [n]}$, we also apply the annealing strategy at the first few epochs.

Combining the sampling scheme (Eq. (3.1)) with the annealing strategy, we obtain the **Evolved Sampling (ES)** framework (formalized in Algorithm Alg. 1).

Algorithm 1 Evolved Sampling (With Pruning)

Require: Dataset $\mathcal{D} = \{z_i\}_{i=1}^n$, optimizer (e.g. Adam)

Require: Pruning ratio r , meta-batch size B , mini-batch size $b \leq B$, total epochs E , annealing epochs $(E_{a_{\text{start}}}, E_{a_{\text{end}}})$, hyper-parameters $\beta_1, \beta_2 \in (0, 1)$

Initialize the scores/weights $s(0) = w(0) = \frac{1}{n} \mathbf{1}_n, t = 0$

for $e = 0, 1, \dots, E - 1$ **do**

if $E_{a_{\text{start}}} \leq e < E - E_{a_{\text{end}}}$ **then**

 Sample a sub-dataset \mathcal{D}_e ($|\mathcal{D}_e| = (1 - r)|\mathcal{D}|$) from \mathcal{D} without replacement, according to the probability $p'_i(e) \propto w_i(e)$ ▷ pruning

else

 Set $\mathcal{D}_e = \mathcal{D}$

end if

for $j = 0, 1, \dots, \lceil \frac{|\mathcal{D}_e|}{B} \rceil - 1$ **do**

 Sample a meta-batch \mathcal{B}_t ($|\mathcal{B}_t| = B$) uniformly from \mathcal{D}_e without replacement

 Compute the loss $\ell_i(\theta(t))$ for $z_i \in \mathcal{B}_t$

 Update score: $s_i(e + 1) \leftarrow \beta_2 s_i(e) + (1 - \beta_2) \ell_i(\theta(t))$ for $z_i \in \mathcal{B}_t$

 Update the weight: $w_i(e + 1) \leftarrow \beta_1 s_i(e) + (1 - \beta_1) \ell_i(\theta(t))$ for $z_i \in \mathcal{B}_t$

if $E_{a_{\text{start}}} \leq e < E - E_{a_{\text{end}}}$ **then**

 Sampling a mini-batch \mathfrak{b}_t ($|\mathfrak{b}_t| = b$) from \mathcal{B}_t without replacement, according to the probability $p_i(e + 1) \propto w_i(e + 1)$

 Update model: $\theta(t + 1) \leftarrow \text{optimizer}(\theta(t); \mathfrak{b}_t)$

else

 Update model: $\theta(t + 1) \leftarrow \text{optimizer}(\theta(t); \mathcal{B}_t)$ ▷ annealing

end if

$t \leftarrow t + 1$

end for

end for

Pruning (optional) Note that applying the sampling scheme (Eq. (3.1)) to meta-batches (with the batch size B) in fact introduces data selection in a *batch* level, since one can always select a smaller batch (with the batch size $b < B$) out of the meta-batch, according to the sampling probability $p_i(t)$ defined in (Eq. (3.1)). For more aggressive data pruning and enhanced data efficiency, we can further extend ES by involving the *set* level data selection. That is, randomly pruning the *whole* dataset according to the probability proportional to the weights $\{w_i(e)\}_{i=1}^n$ at the beginning of the e -th epoch. This is formalized as **Evolved Sampling with Pruning (ESWP)** in Algorithm Alg. 1.

D More Details of Experiments

In this section, we present further experimental results and details. We run all the experiments with one NVIDIA A100 (80GB) with the mixed-precision training except the pre-training of ViT-Large on ImageNet-1K. All the algorithms are implemented based on PyTorch (Paszke et al. [2019]) and Timm (Wightman et al. [2019]). For InfoBatch, our implementation is adapted from Qin et al. [2024].

D.1 Illustrations on Synthetic Datasets

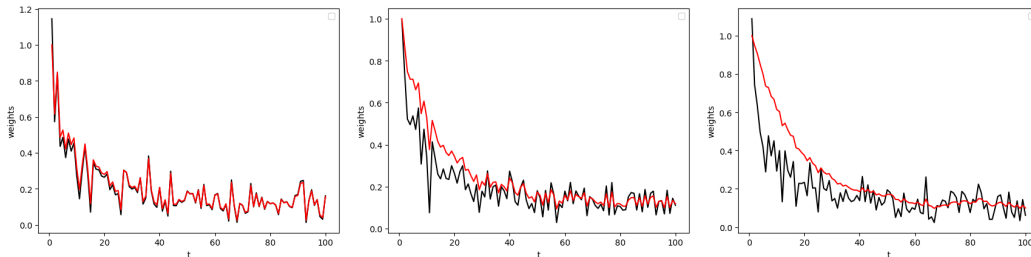


Figure 8: The output weights of different sampling schemes, where the black curves denote (Eq. (2.3)), while the red curves represent (Eq. (3.1)) (from left to right: $\beta_1 = 0.1, 0.5, 0.8$, and $\beta_2 \equiv 0.9$). Here, we draw the black curve as a decayed function with random perturbations, to mimic typical behaviors of loss curves in general machine learning tasks. It is shown that the sampling scheme (Eq. (2.3)) is usually sensitive w.r.t. oscillations. However, when losses oscillate, the sampling scheme (Eq. (3.1)) reacts moderately by not only reserving some portion of dynamical details of losses (high frequencies), but also remaining necessary robustness by capturing the overall trend (low frequencies), with the flexibility to trade off in between by tuning (β_1, β_2) .

D.2 Selected Samples by ES(WP)

D.3 Experiments on CIFAR Datasets

For computer vision (CV) tasks, we train ResNet-18/50 (R-18/50) models on CIFAR-10/100 datasets, using SGD for 200 epochs, with $B = 128/256$ for ResNet-18/50 ($b/B = 50\%$ for ResNet-50).

For the experiments on the CIFAR-10/100 datasets, we use the SGD optimizer with the momentum 0.9 and weight decay 5×10^{-4} . We apply the OneCycle scheduler (Smith and Topin [2019]) with the cosine annealing. For CIFAR-10, the maximal learning rate is 0.2 for the baseline and *set* level selection methods, while 0.05 for *batch* level selection methods due to larger variances of stochastic gradients and 0.08 for ESWP. For CIAFR-100 trained with ResNet-18/50, the maximal learning rates for all the sampling methods are 0.05/0.2, following Qin et al. [2024].

D.4 Experiments of Full Fine-Tuning

Vision Transformer. We finetune ViT-Large model on ImageNet-1K with a meta-batch size $B = 256$ for 10 epochs, using the Adam optimizer with the OneCycle scheduler (Smith and Topin [2019]) with the cosine annealing and a maximal learning rate of 2×10^{-5} .

ALBERT. Following the setup in Xie et al. [2023b] (Table 8), we use the AdamW optimizer and the polynomial decay scheduler with warm up.

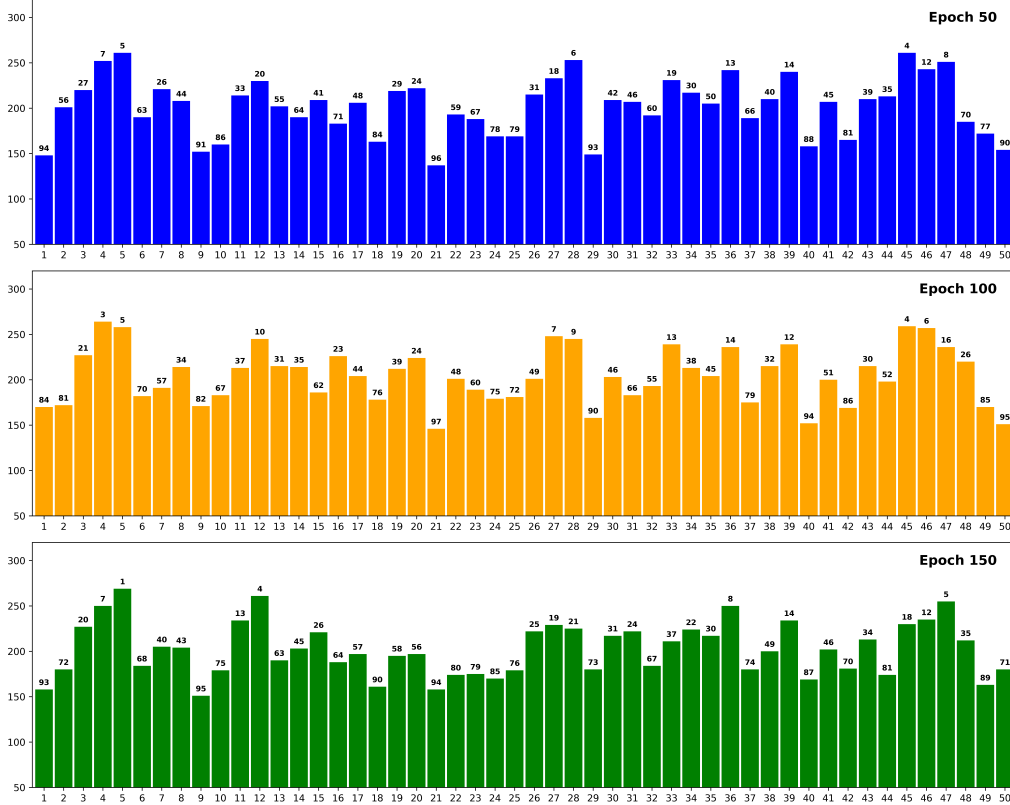


Figure 9: Visualization of the number of selected samples for BP of each class in ESWP (ResNet-50, Cifar-100), following Figure 6 in [Thao Nguyen et al. \[2023\]](#). Here, it shows the result of the first 50 classes. The number on top of each column shows the rank over 100 classes (a lower rank indicates a higher number of selected samples). It is shown that ES(WP) can automatically adjust selected samples at different training stages.

D.5 Experiments of Pre-Training

We conduct the MAE-based pre-training of ViT-Large on ImageNet-1K using $4 \times A100$ GPUs. Following the setup in [He et al. \[2022\]](#), we train for 300 epochs with a 40-epoch warmup, base learning rate 1.5×10^{-4} , weight decay 0.05, and batch sizes $(B, b) = (256, 256)$ per GPU for ESWP, i.e., there is no batch level data selection. In our implementation, the sampling procedure of ESWP is conducted by an additional round of synchronization.

After pre-training, we fine-tune the model for 50 epochs with a 5-epoch warmup, using the standard batched sampling (no data selection) with the batch size $B = 256$ per GPU.

D.6 Experiments on Fine-tuning Qwen

Training Details We conduct experiments on a single A100 (40GB) GPU to investigate the low-resource regime. Our implementation builds upon the verl framework.⁸ We set the batch sizes $B = 32, b = b_{\text{micro}} = 8$, and use the AdamW optimizer with a learning rate of 1×10^{-5} , which follows a cosine decay scheduler with a warm-up ratio of 0.1. We set the total epoch as 10 and evaluate the model after 1K, 2K, and 4K training steps.

Evaluation Details The detailed breakdown of pass@1 results are shown in Tab. 9. We use a temperature of 1.0, top_p=1, the default chat template and Chain-of-Thought (CoT) prompting for evaluation.

⁸<https://github.com/volcengine/verl>

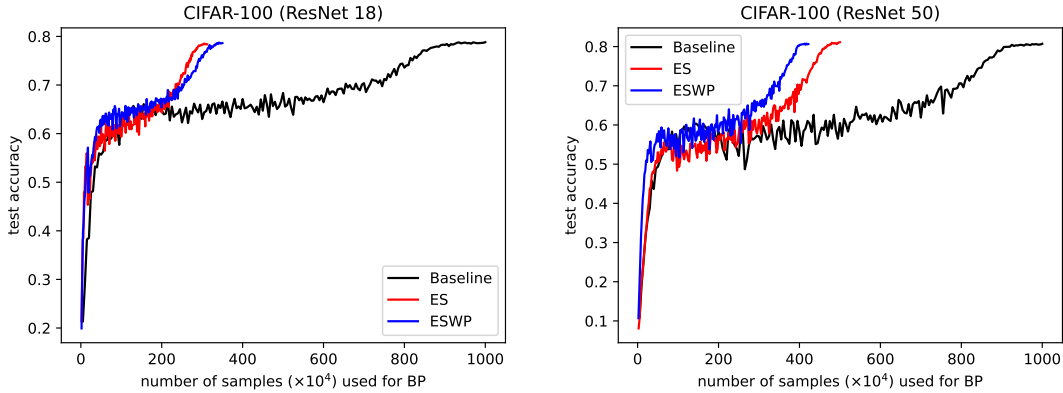


Figure 10: Learning dynamics of different data selection methods: Test accuracy versus the number of samples used for back propagations (BPs).

Table 9: Pass@1 accuracy on MATH500, AIME24, and Olympiad Bench under different training budgets.

Method (Steps, Time)	MATH500	AIME24	Olympiad Bench	Averaged
Baseline (1K, 50min)	61.8	6.7	26.2	31.6
Baseline (2K, 100min)	59.6	10.0	27.7	32.4
Baseline (4K, 200min)	63.4	13.3	25.2	34.0
ESWP (1K, 26.5min)	61.8	10.0	27.4	33.1
ESWP (2K, 53min)	65.2	10.0	28.6	34.6
ESWP (4K, 106min)	65.6	16.7	32.1	38.1

D.7 Comparison Methods: Default Hyper-Parameters

For all the other data selection methods, we also use their default hyper-parameters in original papers in our experiments. Therefore, the comparisons and evaluations are fair in terms of hyper-parameters. We list the default hyper-parameters of all the other data selection methods as follows:

- InfoBatch (Qin et al. [2024]): pruning ratio $r = 0.5$, annealing ratio $1 - \delta = 0.125$;
- KAKURENBO (Thao Nguyen et al. [2023]): pruning ratio $r = 0.3$, confidence threshold $\tau = 0.7$;
- UCB (Raju et al. [2021]): pruning ratio $r = 0.3$, decay parameter $\beta = 0.8$, confidence bound $c = 1$;
- Loss (Katharopoulos and Fleuret [2017]), Order (Kawaguchi and Lu [2020]): the same batch sizes as ES.